Fabrication, characterization, and modeling of electroactive polymer-based strain sensors for wearable applications

DISSERTATION FOR THE DOCTOR OF PHILOSOPHY

Nitin Kumar Singh

STUDENT ID-19899025

GRADUATE SCHOOL OF LIFE SCIENCE AND SYSTEMS ENGINEERING

KYUSHU INSTITUTE OF TECHNOLOGY

WAKAMATSU, KITAKYUSHU, JAPAN

Under the supervision of

PROFESSOR Dr. SHYAM SUDHIR PANDEY

ARISE, AWAKE, AND STOP NOT TILL THE GOAL IS REACHED

(SWAMI VIVEKANANDA)

DEDICATED TO

MY TEACHERS, FAMILY

Those who have the privilege to know have the duty to act, and in that action are the seeds of new knowledge.

(**Albert Einstein)**

Acknowledgements

Here, I would like to express my sincere gratitude to a number of people, without whom it would have not been possible for me to undertake such a novel and huge academic program during my three years in Japan.

First of all, I sincerely thank to my supervisor Professor **Dr. Shyam Sudhir Pandey**, who believed in me and allowed me to do work with him under his esteemed supervision for doctoral program. I would like to express my sincere gratitude to him for his continuous support, encouragement and insightful guidance during my doctoral work. I am very lucky and happy to be able to work with him. When I made mistakes in my work, he expresses his precious understanding and patience. I will never forget his unconditional support and encouragement in and out of the laboratory work to facilitate my stay in Japan. I learned a lot from his knowledge, scientific discussion, keen observation, experience, and philosophy of life which inspired me to strive to be a good researcher as well as molded me into a good human being. I would also like to Prof. Tsuyoshi Hanamoto, Prof. Masaki Fuchiwaki for their kind permission to be in my PhD thesis examination board. At the same time, I am thankful to Prof. Kazuto Takashima for not only being in my PhD thesis examination board but also for allowing me to use his laboratory facility and necessary guidance.

This work has been performed at department of Graduate School of Life Science and Systems Engineering, Kyushu Institute of Technology, Japan. I am very thankful to this university for providing the platform for my research and helping me in managing the necessary criteria for my graduation. I also thank to all student section staffs for helping me in many ways.

I am sincerely thankful to Prof Tomohiro Shibata, who selected me as a PhD candidate under the global advanced assistive robotics (GAAR) program and I would like to thanks Japanese government for selecting me as a MEXT scholar and supported me financially for pursuing PhD from Kyutech. I am also thankful to Dr. Nakajima Hiroshi for their support during my internship at AI and data science department at Omron corporation limited, Kyoto, Japan

Additionally, I want to thank my family members: my mother Brijlesh Singh, my father Raksh Pal Singh, my elder brother Vipin Kumar Singh, my sister Neetu Singh, my niece Aryahi, Aadhya and Anaya, my brother-in law Kapil Kumar and My sister- in- law Nupur Singh who has always loved, supported, and believed in me.

I am also thankful to all lab members who make friendly and nice environment for research. Last but not the least, I owe to God who has always provided me strength, patience and showered his blessings upon me.

Abstract

The last decade has witnessed a shift in the research trends from hard and brittle to soft, flexible, and lightweight wearable devices. There is a fast-growing demand for wearable strain sensors amongst all existing electromechanical soft devices, due to their potential applications in areas like wearable electronics, soft robotics, human motion detection, fitness industries, rehabilitation, and human activity monitoring. Stretchability, sensitivity, life, and repeatability in the wide range are highly desirable for strain sensors. In order to achieve this goal electroactive polymer (EAP) based capacitive strain sensors have been explored as one of the potential candidates for their application in the area of wearable devices.

An electronic type EAP-based strain sensor was fabricated by using silver-coated conductive fabric as an electrode and mixture of silicone rubber as a dielectric film. This sensor was showing linear behaviour but low capacitive range (pF) and less elasticity due to fabric electrode restrict its use in a wide range of applications. To overcome this problem Ionic type of EAP-based strain sensor was fabricated, and efforts were directed to prepare free-standing stretchable polymer films to make capacitance strain sensors while introducing conducting polymers to make hybrid films with controlled conductivity and carbon grease was used as an electrode.

It was found that conducting composite film-based strain sensor can sustain millions of stretching and relaxing cycles, showing high linearity, negligible losses, very high stretchability, and sensitivity. Hyperelastic and viscoelastic modeling have been conducted for estimating different material losses. A crack growth approach has been proposed for predicting the life of the sensor. Complete electromechanical modeling has been proposed for analyzing sensor behavior in 3D space. Further uniaxial tensile testing data was used to estimate different material constants and for predicting sensor behavior in multiaxial loading. Open and fist hand gesture was also recognized.

Table of Contents

CHAPTER-1

INTRODUCTION

1.1 Electroactive polymers

Electroactive polymers (EAPs) are smart polymers whose shape and size change in response to electrical or mechanical stimulation. Electroactive polymers are very light in weight, having high energy density, low losses, easily available, cheap, and highly elastic, and can be stretched up to 400% of the initial dimension. EAPs show electrical, mechanical, tribological, and electromechanical capabilities. Each of these characteristics is important in achieving the targets of actuators, soft electronics, sensors, and generators. EAPs can be classified as electronic EAPs (driven coulomb forces) or ionic EAPs (driven by ionic forces), as given below [1-10].

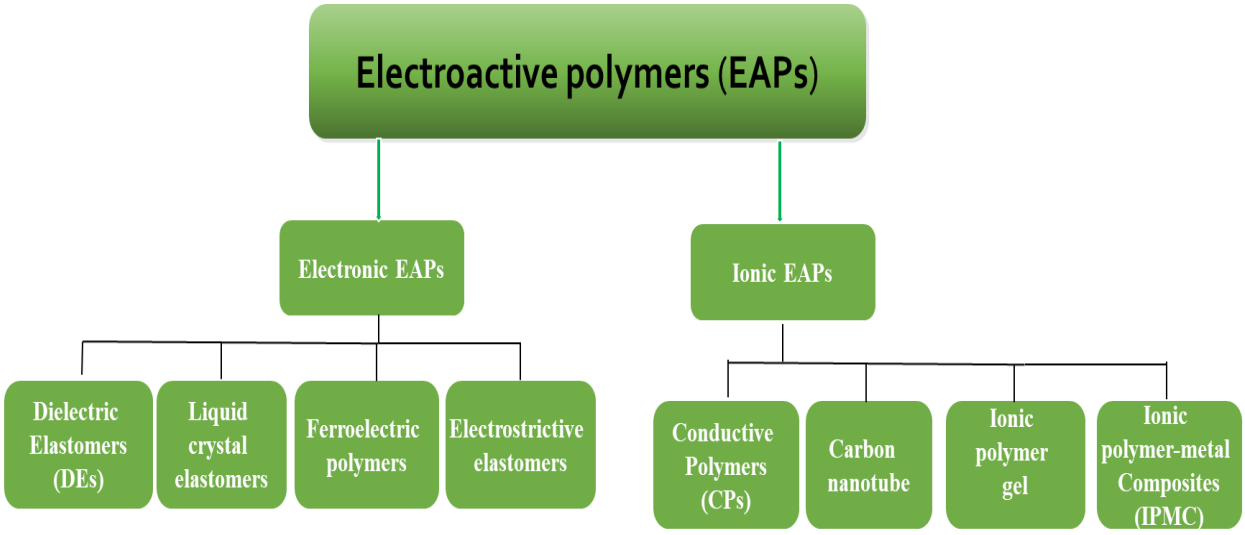

Fig.1: Classification of EAPs

EAPs are mainly known for their applications as actuators, and generators but nowadays these materials are gaining attention as a potential candidate for sensors as well. Due to characteristics like light weight, highly elasticity, large energy density, low viscoelastic losses, having similar properties like human skin, long life, can withstand with high temperature, easily available etc., electroactive polymers have potential to replace traditional sensor technologies which are hard, complex, bulky and not suitable for wearable applications [10-18].

1.1.1 EAPs as an actuator

In actuator mode, EAPs are squeezed between two elastic electrodes and convert electrical energy into mechanical energy, when voltage is applied.

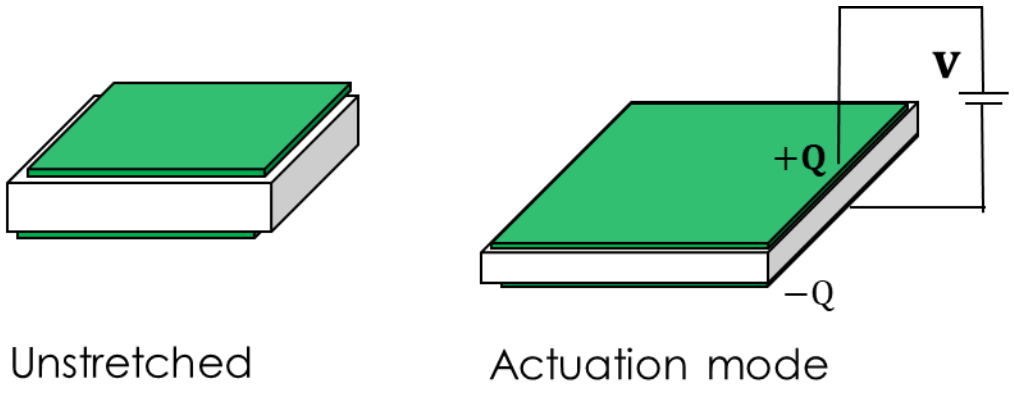

Fig. 2: EAPs as an actuator

On applying voltage area of the whole system increases and the thickness decreases due to the conversion of electrical energy into mechanical energy [19-25]. The actuation phenomenon can be explained by Maxwell's actuation eq. (1), as given below:

$$\sigma = \varepsilon_r \varepsilon_0 \left(\frac{V}{d}\right)^2 \quad (1)$$

where, ε_r is dielectric constant, ε_0 is permittivity of free space = 8.85×10^{-12} F/M, V is applied voltage, d is thickness and σ is Maxwell stress

1.1.2 EAPs as a generator

The basic element of an EAP is an elastically deformable, insulating thin polymer film sandwiched between two compliant electrodes. In generator mode, EAPs can convert the stored mechanical energy into electrical energy. When an electrical charge is placed on the EAP sample and sample is contracted, this lead to shrink in the active area and increment in thickness of the sample [26-35], and if the charge is conserved during this process and mechanical energy decreases consequently electrical energy is generated energy as shown in Fig. 3

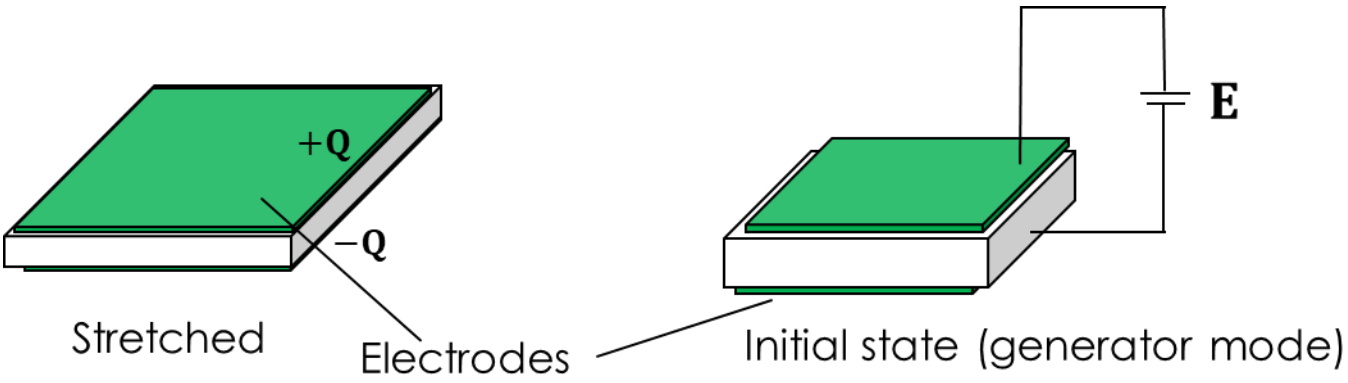

Fig. 3: Operating principle of EAP generators

In generator mode, electrodes act as capacitor plates, and elastomer samples act as a dielectric medium between those plates. So, this EAP film's capacitance varies as it contracts and stretches. The capacitance C of the EAP film-based capacitor can be defined fundamentally as

$$C = \frac{\varepsilon_r \varepsilon_0 A}{d} \tag{2}$$

where, A is active polymer area (coated on each side by electrodes). Then the charge stored (Q_1) in capacitor with V_1 as bias voltage and C_1 as capacitance of the DE film capacitor in pre-stretched state is C_1V_1

Therefore, in stretched state, capacitance C_1 is

$$C_1 = \frac{\varepsilon_r \varepsilon_0 A_1}{d_1} \tag{3}$$

and in relaxed state, capacitance C_2 is

$$C_2 = \frac{\varepsilon_r \varepsilon_0 A_2}{d_2} \tag{4}$$

where A_1 is active polymer area (coated on each side by electrodes), d_1 is thickness of film in pre-stretched state, A_2 is active polymer area (coated on each side by electrodes) and d_2 is film thickness in relaxed state. As discussed earlier as film is contracted the sample area will decrease and thickness will increase thus decreasing the capacitance of film capacitor. In equation shown above since we have $A_2<A_1$ and $d_2>d_1$, we conclude that $C_2<C_1$ and since charge on the film is conserved (constant) then in contracted state it is given as:

$$Q=C_2V_2 \quad (5)$$

where V_2 is the output voltage during state of contraction. From eq. (4) and (5) we can get

$$C_1V_1=C_2V_2 \quad (6)$$

From eq. (2) and (6) we can get

$$V_2 = \frac{C_1V_1}{C_2} = \frac{Q}{C_2} \quad (7)$$

Since charge is conserved in both contracted and stretched condition and $C_2<C_1$, we conclude that $V_2>V_1$ i.e energy been harvested. As we know that stored energy in capacitor is given by

$$E = \frac{1}{2}CV^2 \quad (8)$$

where C is in Farad, V is in volt i.e voltage across the film capacitor and E is in joule i.e stored energy in the capacitor.

The energy harvesting of EAP generator per cycle of operation is given by the difference in the stored energy in contracted state and pre-stretched state. Therefore, this per cycle energy difference can be written as:

$$\Delta E = \frac{1}{2}C_2V_2^2 - \frac{1}{2}C_1V_1^2 \quad (9)$$

From above equation we can conclude easily that ΔE will be positive which shows that energy is generated.

One complete cycle of generation and extracting of electrical energy is from Dielectric elastomers (belongs to electronic type of EAPs family) element through different power electronics converters is called energy harvesting cycle [26-40].

One complete energy harvesting cycle has four states. In first state, Dielectric elastomer (DE) is at relaxed and uncharged. In 2nd state due to stretching DE stores mechanical energy. Charging of DE from external electrical source is occurred from 2nd to 3rd state. From state 3rd to

4th DE comes in its original state and electrical energy is harvested. The output voltage increases from state 3rd to 4th as capacitance decreases while charge is being constant [41-43].

At state 3rd capacitance has highest value while at state 4th minimum value, consequently electrical energy is harvested. It has been reported by many researchers that output amount of electrical energy increases with applied voltage. State from 1st to 4th denotes one complete energy harvesting cycle.

1.1.3 EAP as a sensor

When elastic electrodes are applied on both side of DE film then complete system works as variable parallel plate capacitor. On applying mechanical force, capacitance of this system changes which makes this kind of sensing technology. This change in capacitance can be calibrated for measuring different mechanical quantities like force, pressure, strain etc.: The basic principle of this type of sensing technology may can be seen in the below-mentioned figure, depicts that the capacitance of the entire system changes on stretching (due to changes in area and thickness) [44].

Capacitance of such type of capacitor can be calculated from below mentioned formula:

$$C = \frac{\varepsilon_r \varepsilon_0 A}{d} \qquad (10)$$

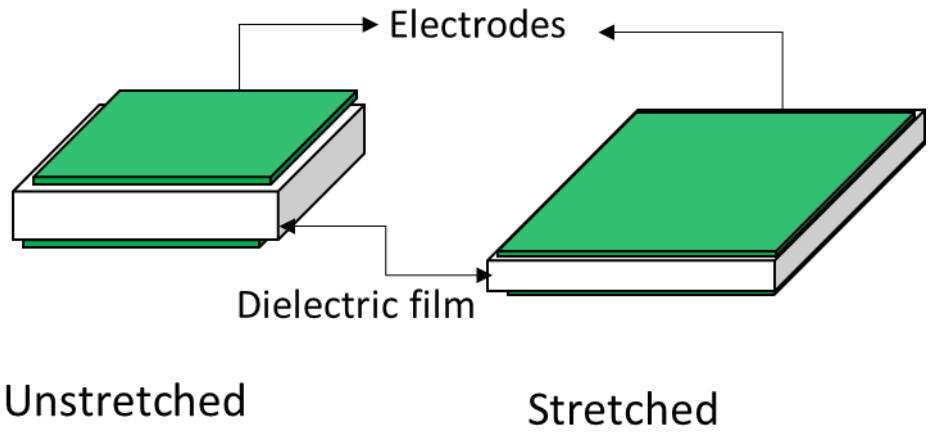

Fig. 4: EAP strain sensor: operating principle

From Fig.4 we can see that on applying mechanical force geometry of sensor varies, which lead to variation in capacitance, makes the base for this type soft senor technology. After removal of mechanical force, sensor comes its original position [45].

1.2 Wearable technologies

Wearable technologies refer to the technology based on electronic devices that can be worn and can be used for a wide range of applications and perform operations beyond the range of traditional systems. Wearable technologies are gaining popularity for improving the lifestyle of human beings. There are a lot of interest in the development of wearables technologies that improve the functionality of devices like medical devices, smart watches, smart glasses, bracelets. Actuators, sensors, and energy harvesters build-in smart wearable electronic devices can be used in medical, healthcare, sports, fitness, data acquisition, and entertainment fields. The growing interest in healthcare development and improvement of such intelligent devices, especially sensing technologies used in garments with real-time monitoring and gesture recognition can be a key factor in transforming the healthcare, sports, fitness, medical industry, and human-machine interface. Wearable devices can be used to monitor the activity of old people, patients with chronic illnesses, and athletes. These devices can also be used in daily life to assist doctors and nurses in monitoring patients at home [46].

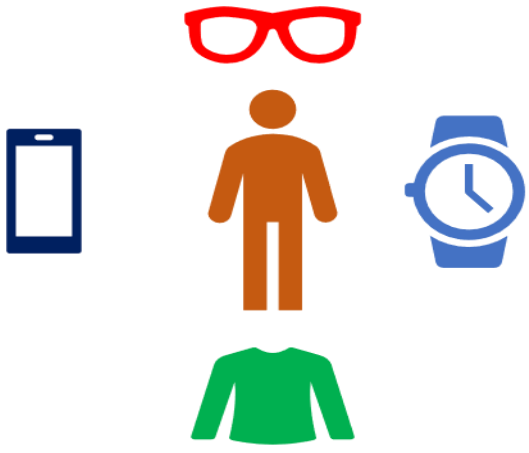

Fig. 5: Wearable technology

1.2.1 Wearable sensing mechanism

A wearable system consists of sensors embedded directly into clothes or in patches or bandages that can be worn under clothes and connected to a PC or mobile via wireless or bluetooth.

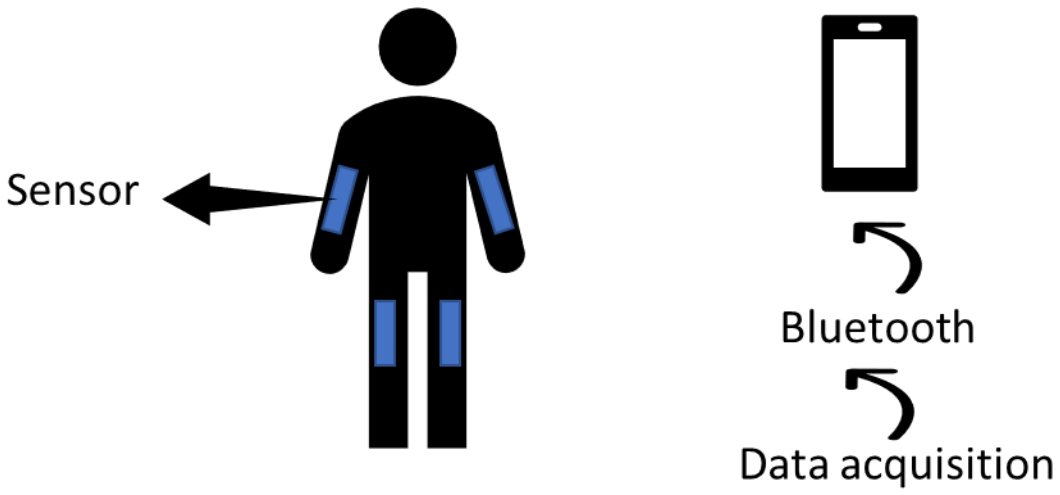

Fig. 6: Wearable system for human activity monitoring

Using a wireless LAN or an internet connection, you can connect to a database server. Data gathered by using these techniques can be used to predict possible patient deterioration in real-time. Clinical situation can be analyzed to see if a clinical intervention has any effect. These kinds of systems can also be used sport and fitness industry for giving user, information regarding their correct body posture. Wearables systems can also be used in rehabilitation process, gesture recognition and for remotely monitoring of human activities. So, it can be concluded that wearables system can play an important role in human machine interaction, can make technology more advanced and can improve the life of common people directly [47].

1.2.2 Wearable strain sensors

Metal foil-based resistive-type strain sensors were firstly introduced which can detect small strain (up to 5%), such as small and rigid bodies deformations. Nowadays the need for wearable devices

has been shifted from brittle to flexible devices. In most cases, stretchable strain sensors are made of polymers, conducting nano materials, conductive yarns/fabrics, composites, thin film etc [48]. Basically, wearable strain sensors can be categories into two types, one is resistive based strain sensors and another is capacitive based strain sensors. Both types of sensors have been explained below. From below mentioned formula we can easily measure change in resistance with strain

$$R = \rho \frac{l}{A} \tag{11}$$

where, R is resistance; ρ is resistivity; l is length; and A is area.

Wearable capacitive-type strain sensors are frequently made by squeezing a dielectric layer between two elastic electrodes. Dielectric medium does not let the charge pass from one electrode to another, thus the whole system works as a variable parallel plate capacitor and capacitance (C) of such type of a system can be defined by below mentioned expression:

$$C = \frac{\varepsilon_r \varepsilon_0 A}{d} \tag{12}$$

These types of sensor's capacitance vary with the strain which makes the sensing mechanics. Resistive and capacitive strain sensors have been widely researched in recent years for wearables

Table 1: Comparison for different types of strain sensors [49]

Sensing materials	Transduction principle	Elasticity	Gauge factor	Linearity	References
CNT/PDMS	Resistive	30%	6436	Linear	[28]
Acrylic elastomer/liquid metal	Capacitive	50%	1.61	Linear	[29]
CB/PDMS	Resistive	30%	29.1	Linear	[30]
Ecoflex/AgNWs	Capacitive	50%	0.7	Linear	[31]
Rubber/polydopamine	Resistive	180	346	Non-linear	[32]
AgNPs/graphene/TPU	Resistive	1000	7-476	Nonlinear	[33]
Liquid metal/PDMS	Resistive	13.3	3.53	Linear	[34]
Ti3C2TxMXene/CNT	Resistive	130	4.4-772.6	Non-linear	[35]
Nitin et al	Capacitive	150%	4 at 100% strain	Linear	

In above table different types of resistive and capacitive sensors have been compared.

1.3 Existing issues and research motivation

Wearable devices have the potential to push the limits of human-technology interaction. Most people are familiar with smart gadgets like fitness monitors and smart watches that provide basic data like heart rate and steps taken. These technologies, on the other hand, continue to rely on traditional electronics with rigid components. Components that can offer accurate, dependable data without inhibiting natural mobility are in higher demand. Soft, stretchable sensors have attracted a lot of attention as these sensors can retain sensitivity and conformability to the body even at large deformation.

Soft sensors respond quickly and can be fabricated easily, make them a potential candidate for wearables. Wearable sensors are being widely used in detecting motion, health monitoring, rehabilitation, can play an important role in human-machine interface.

Mainly resistive and capacitive based sensors are widely used. Resistive type sensors have good sensitivity as gauge factor of these sensors is very high but resistive sensors are not suitable in wearables due to nonlinearity. Electrical resistance measurement shows linear behaviour at small strain, but non-linear at large deformation, due to transient changes in resistivity & geometric influences. On the other hand, capacitive sensors show linear characteristics even at large strain but gauge factor (sensitivity) and base capacitance of these sensors is very low, consequently now a days researchers are trying to increase the gauge factor and base capacitance of capacitive based sensors. One more challenge of capacitive sensor is to choose a suitable electrode in terms of high life and, whose conductivity could withstand even at large deformation. At the same time, it could be easily embedded into clothes for making a wearable system, therefore, we feel that there is a lot scope and room is still available for conducting research in this area. In order to overcome the above-mentioned drawbacks, the objective of this thesis is to find a suitable capacitive-based wearable strain sensor, relatively unaffected by transient changes in electrode resistance and shows high base value of capacitance, high strechability, durability and linear behavior even at large values deformation.

1.4 Organization of thesis

The thesis consists of six chapters. 1st chapter explains the different types of electroactive polymers and their potential applications in wearable technologies. Later working principle of operation and involved components of wearable technology have been explained. This chapter also gives an overview of different types of strain sensors, and their working, pros, and cons have been discussed in detail along with the aim and motivation for the thesis.

2nd chapter deals with details about necessary materials like elastomers, electrodes, experimental set-up, uniaxial tensile test protocol, dimension and type of specimen, and involved techniques for post-processing of experimental data used for the entire research work carried out during the doctoral course.

3rd chapter explains the fabrication of an electronic type of electroactive polymer (EAP) based strain sensor. Highly stretchable silicone rubber and carbon nano tube (CNT)-based dielectric film was used. This composite dielectric film was sandwiched between the conducting and stretchable silver-coated fabric-based upper and bottom electrodes and whole system works as a capacitive based strain sensor. Uniaxial tensile tests were performed for mechanical characterization of the sensor, further first half cycle of stress-strain curve was validated with constitutive equations. Hyper elastic and viscoelastic modeling were conducted for understanding the sensor behavior. Sensor was showing negligible viscoelastic losses until 100% of strain value. Stress strain curve was showing good agreement with the second-order Ogden model (for 100% of strain value), further fitting parameters were obtained and complete modeling has been proposed for predicting the sensor`s behavior in multiaxial loading. At 150 % value of strain, sensor was showing viscoelastic behavior which has been analyzed by using Prony series based viscoelastic model. Computer controlled and mobile X-Y electrometer was used for measuring capacitance for multiple loading and unloading cycles at different value of strain. Complete electromechanical modeling was proposed and during the relaxing and stretching cycle to see how different mechanical parameters vary in 3D space was also discussed in brief.

4th chapter includes fabrication, modeling and characterization of ionic type of EAP based strain sensor. Styrene-ethylene-butylene-styrene (SEBS) rubber and dodecyl benzenesulfonic acid (DBSA) doped polyaniline composite was used for fabricating the conducting and stretchable freestanding dielectric films for ionic EAP based strain sensor. Carbon grease was used as an electrode material. Various existing mathematical models were used for analyzing stress-strain curves obtained from uniaxial tensile testing for predicting the mechanical behavior of the sensor. The sensor was showing hyperelastic behavior and viscoelastic losses can be neglected. Crack growth-based approach has been developed for predicting the life of sensor and it was found that sensor can sustain millions of cycles. Further tear strength of sensor was also estimated by tensile testing of trouser type of specimen and it was found that material has a good tear strength (150N/mm,), which also confirm that sensor has long life (in millions).

In chapter 5th applications of EAPs-based strain sensors have been discussed in wearables. The sensor was fixed on the elbow joints and a relationship (linear) has been developed between joint angle and capacitance. Graph was plotted between capacitance and joint angles by using linear equation. With the help of this linear equation, position of elbow can be predicted by measuring capacitance at that joint angle. Elbow was bent from 0 to 90 degree and then 90 to 0 degree (a protractor was used to measure the angle of the arm) and capacitance during bending and straightening state of elbow was measured by using electrometer. By using LEAP technology's sensor kit graph between capacitance and time was plotted for multiple cycles. Using this sensor kit data was collected for recognizing open and fist hand gesture.

Finally, last and 6th chapter summarizes the general conclusion of the whole thesis along with the outlooks and future prospects of the present work. In future, different types of hand gesture recognition and fabrication of composite electrode has been suggested for using it on ionic electroactive based strain sensors.

1.5 References

(1) C. Balazs, R. Van, P. Bauer, J. Abraham, and A. Wattez; "Energy harvesting using dielectric elastomers". In *Power Electronics and Motion Control Conference (EPE/PEMC), 14th International*, pp. S4-18. IEEE, 2014.

(2) Wang, Wei, P. He, S. Soekamtoputra, F. Choi, G. Kang, and S. Kim; "Dielectric Electroactive Polymer energy harvesting system forward path design for different vibration input patterns". In *Electro/Information Technology (EIT), 2011 IEEE International Conference on*, pp. 1-6. IEEE, Feb, 2014.

(3) P. Mitcheson et al., "Energy harvesting from human and machine motion for wireless electronic devices," Proceedings of the IEEE, vol. 96, no. 9, pp. 1457 –1486, Sept. 2013.

(4) M. Rofouei et al., "Optimization intensive energy harvesting," pp. 272–275. IEEE, 2013.

(5) T. McKay et al., "Self-priming dielectric elastomer generators," Smart Materials and Structures, vol. 19, p. 055025, 2013.

(6) S. Roundy, P.K. Wright, and J. Rabaey; "*Energy Scavenging for Wireless Sensor Networks with Special Focus on Vibrations"*, Kluwer Academic Press, 2012.

(7) R. D. Kornbluh, J. Eckerle, and B. McCoy A scalable solution to harvest kinetic energy, SPIE Newsroom. DOI: 10.1117/2.1201106.003749,18 July 2013.

(8) Due, Jens, R. Nielsen. "Energy harvesting with di-electro active polymers". In *Power Electronics, Machines and Drives (PEMD 2010), 5th IET International Conference on*, pp. 1-6, IET, 2010.

(9) Paradiso and T. Starner; "Energy scavenging for mobile and wireless electronics". *Pervasive Computing, IEEE* 4, no. 1, pp: 18-27. *Published by the IEEE CS and IEEE ComSoc* 1536-1268/05, 2005.

(10) S. Nielsen et al. "Energy harvesting using electroactive polymer". In Power Electronics, Machines and Drives, 7th *IET* International Conference on, pp. 1-8. *IET*, 2012.

(11) Sodano et al. “A review of power harvesting from vibration using piezoelectric materials”. Shock and Vibration Digest 36, no. 3: 197-206, 2004.

(12) R.Kornbluh, R. Perline, Q. Pei, R. Heydt, S. Stanford, S. Oh, J. Eckerle. Electroelastomers: Applications of Dielectric Elastomer Transducers for Actuation, Generation and Smart Structures, Sri International, pp. 2-5, 2001.

(13) Koh, S. Adrian, C. Keplinger, T. Li, S. Bauer, and Z. Suo. “Dielectric elastomer generators: How much energy can be converted?” Mechatronics, *IEEE/ASME Transactions* on 16, no. 1: 33-41, 2011.

(14) K. Liang, F. Hofmann Member *IEEE* Yiming Liu, Student Member and *IEEE* Q. Zhang, Senior Member. Investigation of electrostrictive polymers for energy harvesting. *IEEE transactions on ultrasonic,ferroelectrics, and frequency control,* 52, 2005.

(15) S. Jin et al., “Dielectric Elastomer Generators” , SPIE vol 124,pp 1-8, 2010

(16) R. perline “Dielectric elastomer: generator mode fundamentals and aplications” SRI internatonals, 333 menlo park,CA 94025,2011.

(17) Pramanik, B., Sahu, R. K., Bhaumik, S., Patra, K., Pandey, A. K., & Setua, “Experimental study on permittivity of acrylic dielectric elastomer”. In *Properties and Applications of Dielectric Materials (ICPADM), 2012 IEEE 10th International Conference on the* (pp. 1-4). IEEE, 2012.

(18) Pelrine, Ron, R. Kornbluh, J. Eckerle, P. Jeuck, S. Oh, Q.Pei, and S. Stanford. “Dielectric elastomers: Generator mode fundamentals and applications”. In *Proc. SPIE*, vol. 4329, pp. 148-156. 2001.

(19) Koh et al., “DEG: How much energy can be converted?” *IEEE/ASME Transactions on Mechatronics*, vol.16, no.1, pp.33-41, Feb. 2011.

(20) Carpi et al.,”Dielectric Elastomers as Electromechanical Transducers Fundamentals, Materials, Devices, Models and Applications of an Emerging Electroactive Polymer Technology, ISBN: 978-0-08-047488-5 2008, Pages 3,2011.

(21) Chiba et al., “Consistent ocean wave energy harvesting using electroactive polymer (dielectric elastomer) artificial muscle generators”. *Applied Energy* 104: 497-502, 2013.

(22) R. Pelrine, et al. “DEG mode fundamentals and applications”, *Smart Structures and Materials 2004: Electroactive Polymer Actuators and Devices,* 2004.

(23) S. Chiba, M. Waki, R. Kornbluh, R. Pelrine, “Innovative power generators for energy harvesting using electroactive polymer artificial muscles”, *Electroactive Polymer Actuators and Devices (EAPAD) , Proceedings of the SPIE*, vol. 6927, 2008.

(24) Chiba, Seiki, and Mikio Waki. "Extending applications of dielectric elastomer artificial muscles to wireless communication systems." *InTech, Rijeka, Croatia,* 2011.

(25) Chiba, Seiki, Mikio Waki, K.Masuda, and T. Ikoma. "Current status and future prospects of electric generators using electroactive polymer artificial muscle." In *OCEANS 2010 IEEE-Sydney*, pp. 1-5. IEEE, 2010.

(26) H. Prahlad, R. Kornbluh, R. Pelrine, S. Stanford, J. Eckerle, S. Oh, “Polymer power: dielectric elastomers and their applications in distributed actuation and power generation”, *International Conference on Smart Materials Structures and Systems 2005*, pp. SA-100–SA-107, 2005.

(27) R. Kessel, B. Czech, P. Bauer, J. A. Ferreira, "Optimizing the dielectric elastomer energy harvesting cycles", *IECON 2010*, pp.1281-1286, 2012.

(28) J. A. Paradiso and T. Starner, “Energy scavenging for mobile and wireless electronics,” IEEE Pervasive Computing, vol. 4, no. 1, pp. 18–27, Jan**. 2005.**

(29) R. D. Kornbluh et al., “From boots to buoys: promises and challenges of dielectric elastomer energy harvesting,” Polymer, vol. 7976, no. 1, pp. 797 605–797 605–19, 2011.

(30) Dimopoulos, Trintis, and S. Munk. "Comparison of the DEG polymer generator energy harvesting cycles." *SPIE* Smart Structures, Materials and Nondestructive Evaluation and Health Monitoring. International Society for Optics and Photonics, 2012.

(31) J. B. Wendt et al., “Spatiotemporal assignment of energy harvesters on a self-sustaining medical shoe,” in Sensors, 2012 IEEE, Oct. 2012.

(32) T. Wacharasindhu and J. W. Kwon, "A micromachined energy harvester from a keyboard using combined electromagnetic and piezoelectric conversion," Journal of Micromechanics and Microengineering, vol. 18, no. 10, p. 104016, 2008.

(33) V. Raghunathan, A. Kansal, J. Hsu, J. Friedman, and M. Srivastava, "Design Considerations for Solar Energy Harvesting Wireless Embedded Systems," *IEEE 4th International Symposium on IPSN*, pp. 457 – 462, 15 Apr 2005.

(34) G.K. Ottman, H.F. Hofmann, and G.A. Lesieutre, "Optimized piezoelectric energy harvesting circuit using step-down converter in discontinuous conduction mode." *IEEE Trans on Power Elect*, vol.18, no.2, pp.696-703, 2003.

(35) A.C. Bhatt et al., "Adaptive Piezoelectric Energy Harvesting Circuit for Wireless Remote Power Supply," *IEEE Trans on Power Elec*, Vol 17, no. 5, pp. 669-676, 2002.

(36) D. Guyomar, A. Badel, E. Lefeuvre, and C. Richard, "Toward Energy Harvesting Using Active Materials and Conversion Improvement by Nonlinear Processing,"_*IEEE Transactions on Ultrasonics, Ferroelectrics, and Frequency Control*, vol. 52, no. 4, Apr 2005.

(37) S. Roundy, E.S. Leland, J. Baker, E. Reilly, E. Lai, B. Otis, J.M Rabaey, P.K. Wright "Improving Power Output for Vibration-Based Energy Scavengers," Pervasive Computing, *Published by the IEEE CS and IEEE ComSoc 1536-1268*, pp. 28-36 January-March 2005.

(38) M. Ericka, D. Vasic, F. Costa, G. Poulain "Predictive Energy Harvesting from Mechanical Vibration Using aCircular Piezoelectric Membrane." *IEEE UltrasonicsSymposium*, pp. 946-949, 2005.

(39) McKay, T. G. Benjamin, M. Obrien, E. Calius, and I. A. Anderson. "Soft generators using dielectric elastomers." *Applied Physics Letters* 98, no. 14: 142903-142903, 2011.

(40) H.Lee, Ran, M. Lyu, E. Kim, and C. Nah. "Fabrication and performance of a donut-shaped generator based on dielectric elastomer." *Journal of Applied Polymer Science* 2013.

(41) M. Fontana, G. Rosati, and M. Bergamasco. "Oscillating-water-column wave-energy-converter based on dielectric elastomer generator". In *SPIE Smart Structures and Materials+*

Nondestructive Evaluation and Health Monitoring, pp. 86870I-86870I. International Society for Optics and Photonics, 2013.

(42) Anderson, Iain A., Ioannis A. Ieropoulos, T. McKay, B. O'Brien, and Chris Melhuish. "Power for robotic artificial muscles." *Mechatronics, IEEE/ASME Transactions on* 16, no. 1: 107-111, Published on 2011.

(43) Ozlem, Kadir, et al. "Textile based sensing system for lower limb motion monitoring." *International Conference on NeuroRehabilitation*. Springer, Cham, 2018.

(44) Wang, Jilong, Chunhong Lu, and Kun Zhang. "Textile-based strain sensor for human motion detection." *Energy & Environmental Materials* 3.1 (2020): 80-100.

(45) Beccai, Lucia, et al. "Soft robotics mechanosensing." *Soft Robotics: Trends, Applications and Challenges*. Springer, Cham, 2017. 11-21.

(46) ouri, Hamid, et al. "Wearable and stretchable strain sensors: materials, sensing mechanisms, and applications." *Advanced Intelligent Systems* 2.8 (2020): 2000039.

(47) Huang, Bo, et al. "Wearable stretch sensors for motion measurement of the wrist joint based on dielectric elastomers." *Sensors* 17.12 (2017): 2708.

(48) Thao et al "Tuning Electromechanical Performance in Wrinkled Thin Film Soft Strain Sensors for Wearable Applications" 2020, Ph.D. thesis

(49) Singh, Nitin Kumar, Kazuto Takashima, and Shyam S. Pandey. "Fabrication, characterization and modelling of the fabric electrode-based highly stretchable capacitive strain sensor." Materials Today Communications 32 (2022): 104095.

CHAPTER-2

MATERIALS AND METHODS

2.1 Materials used

For electronic type EAP based strain sensor's fabrication, elastic conducting fabric (YSILVER83) consisting of silver coated textile was purchased from YL Machinery, China and Silicone rubber (EcoflexTM 00-30) was used as a dielectric film. Carbon nano tube (CNT) was purchased Carbon Nanotechnologies Inc, USA. Digital electrometer (Advantech model 8252) was used to measure the capacitance of sensor. Our in-house developed system consisting of a computer-controlled X-Y stage controller (Mark-102, Sigma Koki, Japan), load cell (LU-10K, Kyowa) and digital Oscilloscope (TDS 2001C, Techtronic, USA) was used to uniaxial tensile testing for multiple loading and unloading cycles. Sheet resistivity meter was purchased from Mitsubishi chemical corporation (model no MCP-T610).

For fabrication ionic type of EAP based strain sensor Polystyrene-block-poly(ethylene-ran-butylene)-block-polystyrene-graft-maleic anhydride (SEBS-g-MA) was purchased from the Sigma-Aldrich co. and used for the fabrication of the composite film using DBSA (dedocyl benzene sulfonate acid) doped Polyaniline (PANI) composite film. Composite stretchable film was prepared by casting from the toluene solutions (at different concentrations) on glass disc. Edge crack specimen and trouser type of specimen were prepared from DBSA doped polyaniline-SEBS rubber composite film.

2.2 Uniaxial tensile testing machine

Uniaxial tensile machine (UTM) is generally used for understanding the mechanical properties of isotropic materials and specimen is subjected under controlled load. Results obtained from tensile testing machine can be used for analyzing stress strain behavior, which play a significant role in material selection for desirable application.

From these measurements' material properties like cyclic stress-softening, elastic limit, elongation, Mullins effect, modulus, ultimate tensile strength, stress strain analysis can be analyzed by performing uniaxial tensile test [1].

Tensile testing system used in this work has been shown in Fig. 1. It consists 100N load cell, stage controller, digital oscilloscope. Rectangular, trouser, edge crack type specimen was used for tensile testing.

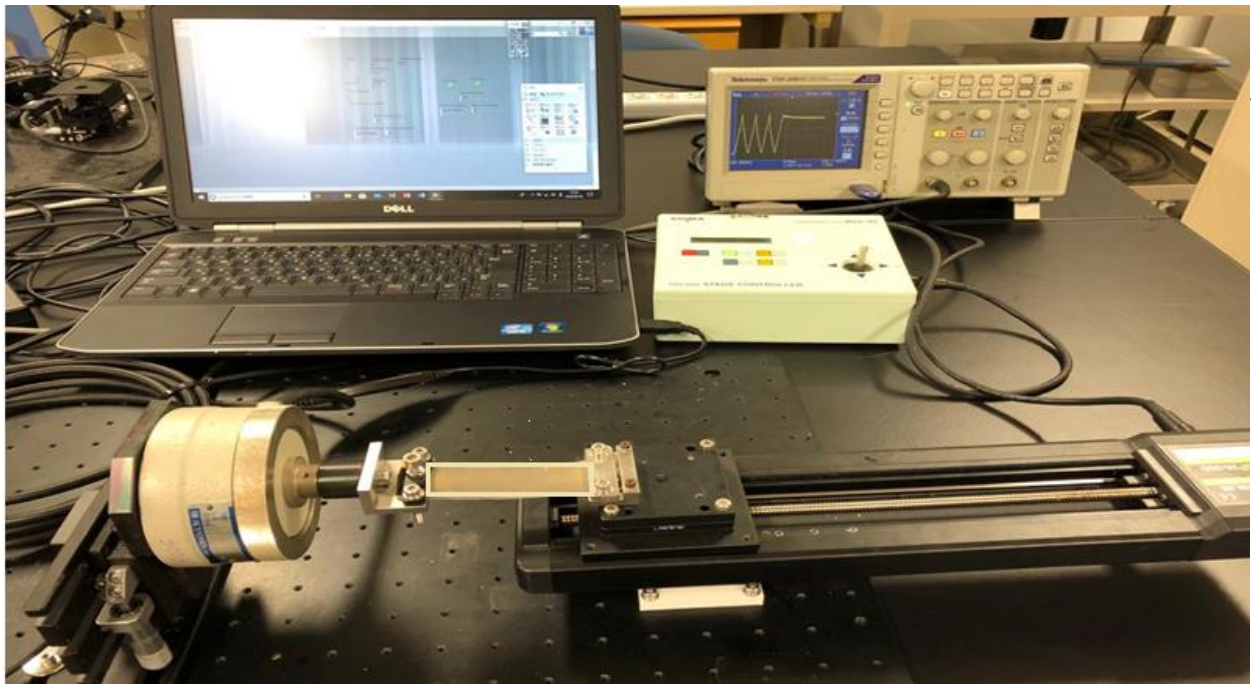

Fig. 1: Uniaxial tensile testing set-up

After running tensile tests by using different type of samples, recorded force and displacement data was further analyzed by a stress-strain curve, which was constructed using the following relations [4]:

$$\sigma = F/A = \frac{\partial W}{\partial \lambda} \quad (1)$$

$$A = wt \quad (2)$$

$$\varepsilon = \Delta L/L \quad (3)$$

$$\lambda = 1+\varepsilon \quad (4)$$

Where, σ, ε, ΔL, L and λ, F, A, W, w, t are stress, strain, change in length, original length, extension coefficient, force, cross-sectional area, strain energy density, width of the specimen, thickness respectively.

2.3 Scanning Electron Microscope (SEM)

To understand the effect of stretching on the electric characterization of the conductive fabric electrodes and percolation of the silver on the fabric yarns, scanning electron microscopic (SEM) analysis of fabric electrode under normal and stretched state (at 150% strain) was conducted.

Fig. 2: Scanning electron microscope (SEM)

The SEM consists of a backscattered electron detector (BED), an upper electron detector (UED), an upper secondary electron detector (USD), and a lower electron detector (LED). By changing the filter voltage, USD and BED can be changed for UED. The acquisition of 3D images is allowed by LED [2].

2.4 Sheet resistivity meter

Electrical characterization of conductive fabric was performed by measuring the sheet resistivity of the film at the different strain values. Four-point probe-based sheet resistivity meter was used

for measuring sheet resistivity at different strain values. Sheet resistivity is measured in ohm/square by passing current through the two outer probes and measuring the voltage across the two inner probes [3].

Fig. 3: Sheet resistivity meter

Sheet resistivity is normally expressed in ohm/ square. A square conductive sheet's resistance remains constant regardless of its size as long as it remains square. Sheet resistivity can be calculated by ρ/t where ρ is resistivity and t is thickness of film.

2.5 Electrometer for measuring capacitance

An electrometer is a device that measures the electric charge or potential difference between two points [4]. computer-controlled and programable electrometer (Advantech 8512) was used for measuring the capacitance of different types sensors used in this thesis.

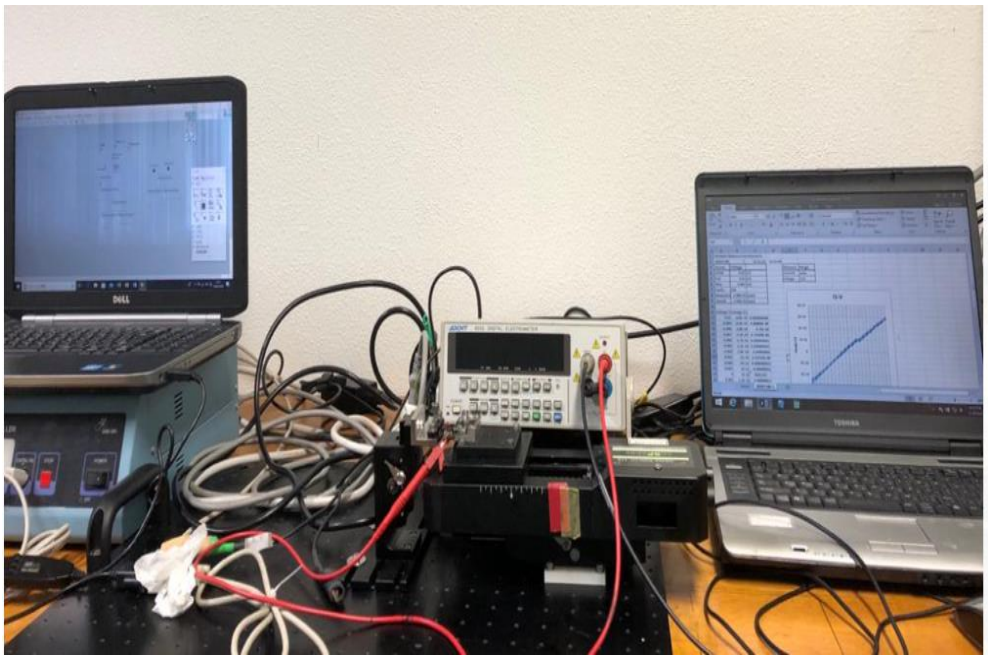

Fig. 4: Electrometer based capacitive measuring set up

Positive and negative probe of the electrometer was connected through upper and lower electrode of the sensor through conducting carbon tape. Capacitance change was measured for multiple loading and unloading cycles at different strain level by experimental setup shown in above figure.

2.6 Film fabrication method:

Block diagram representation of fabrication process of composite film for electronic EAP based strain sensor is given below:

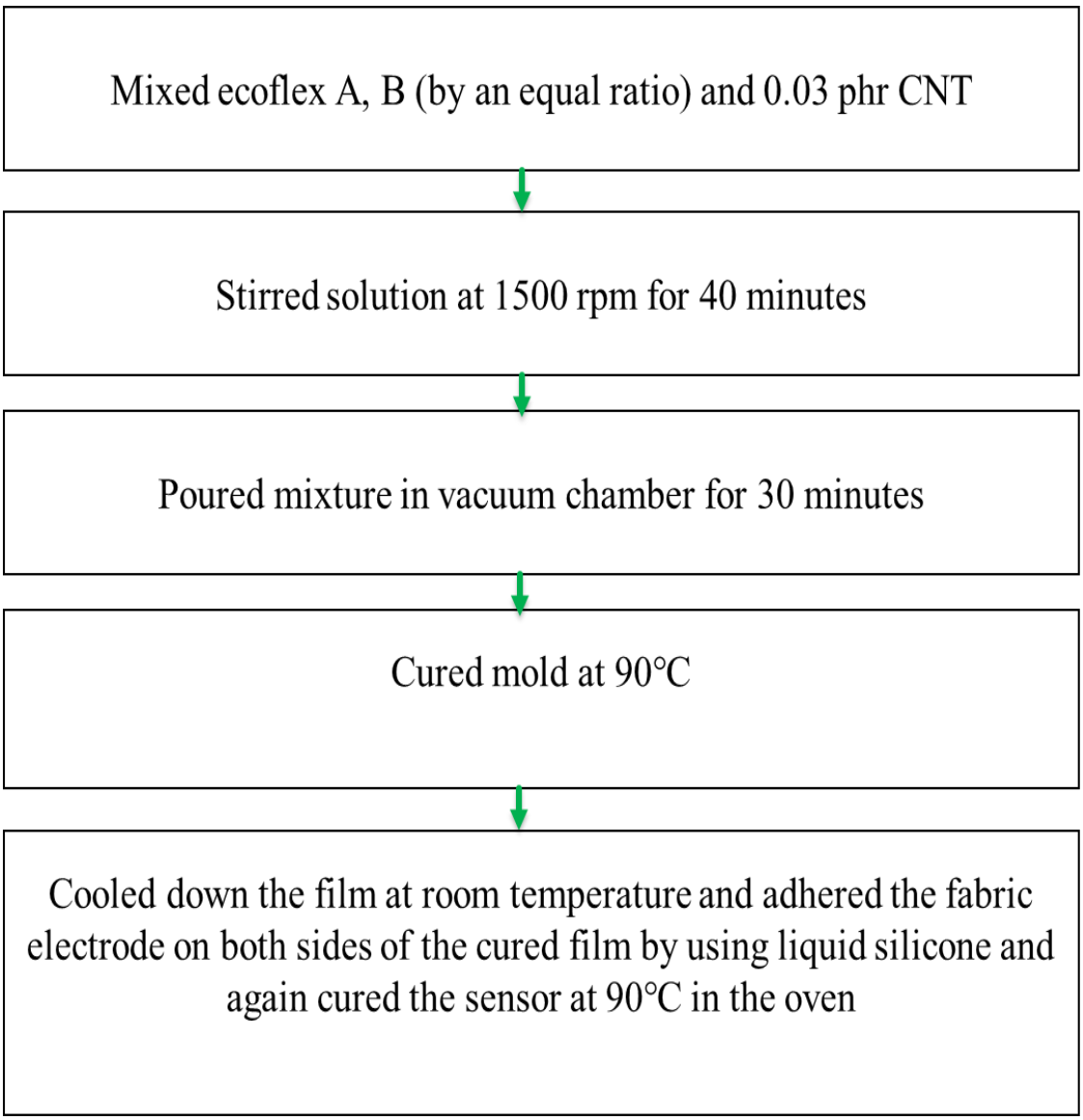

Fig. 5: Fabrication process of electronic type of EAP based strain sensors

Block diagram representation for fabricating DBSA doped Ionic type of EAP based strain sensor is given below:

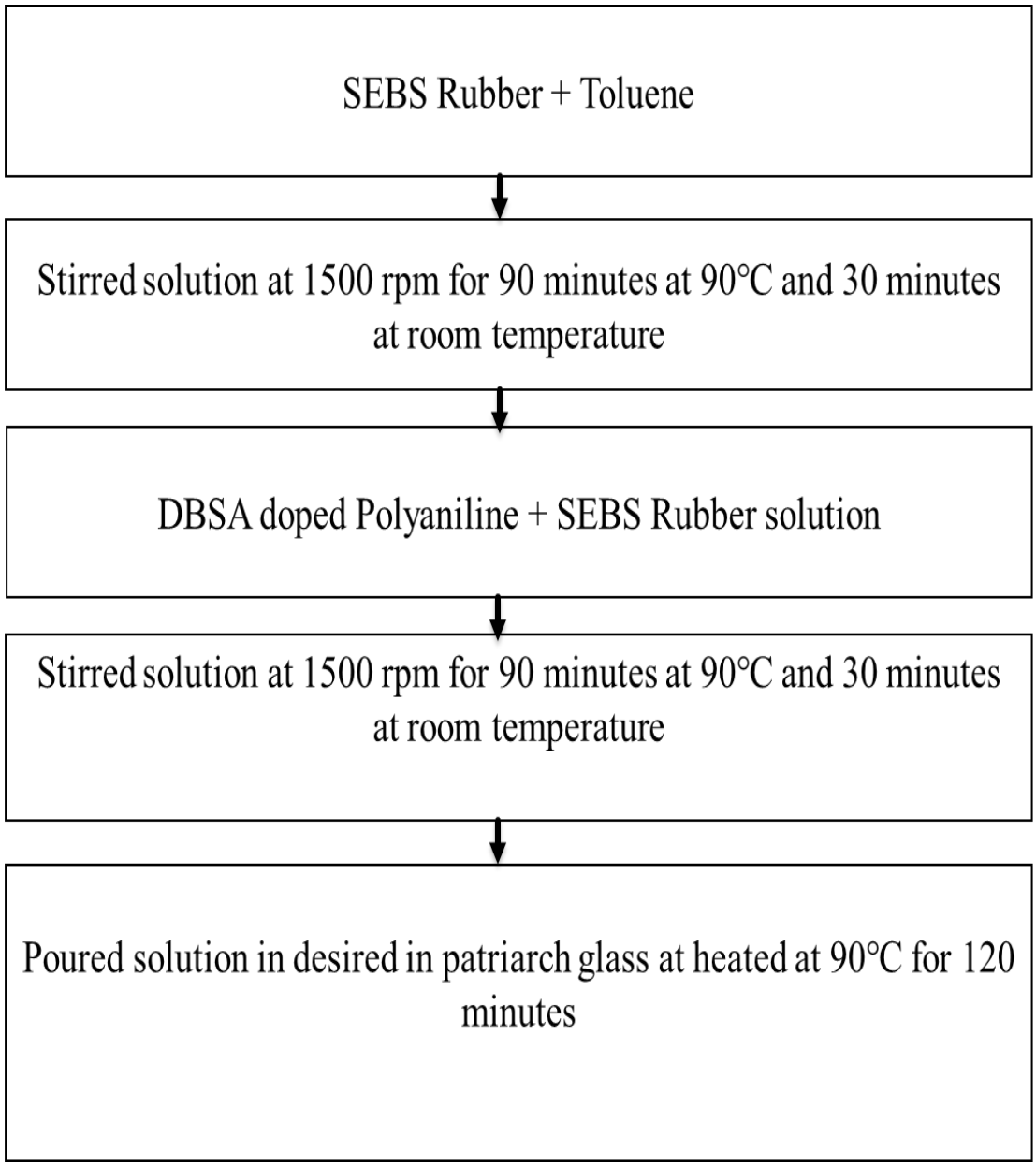

Fig. 6: Steps involved in fabrication process of Ionic type of EAP based strain sensors

2.7 References

1. Hu, Jianhui, et al. "Epoxy shape memory polymer (SMP): material preparation, uniaxial tensile tests and dynamic mechanical analysis." Polymer Testing 62 (2017): 335-341.

2. Seiler, H. "Secondary electron emission in the scanning electron microscope." Journal of Applied Physics 54.11 (1983): R1-R18.

3. Zrudsky, Donald R., Harry D. Bush, and John R. Fassett. "Four point sheet resistivity techniques." Review of Scientific Instruments 37.7 (1966): 885-890.

4. Gunn, Ross. "Principles of a new portable electrometer." Physical Review 40.2 (1932): 307.

CHAPTER-3

FABRICATION, CHARACTERIZATION AND ELECTROMECHANICAL MODELLING OF THE ELECTRONIC ELECTROACTIVE POLYMER BASED STRAIN SENSOR

3.1 Introduction

The research trends have recently shifted from rigid and heavy devices to flexible, soft, and less heavy devices. dielectric elastomers (DEs) strain sensors can be a good choice for electromechanical sensing devices used in soft robotics, healthcare, augmented reality, and wearable sensors [1]. Recently researchers introduced a silicone-based capacitive sensor array that can be used for motion capture and stretch sensing [2]. Additionally, capacitive-based elastomeric sensors that can measure compressive strain as well [3]. Ionic electroactive polymer-based strain sensors having large base capacitance values were also introduced by Nitin et al. [4].

Dielectric elastomers have better possibility for a sensing mechanism as DEs have low moduli and can be deformed in any direction [5]. Plenty of researchers worked on silicone-based composite film to fabricate resistive-type sensors. A graphene-carbon black-silicone rubber composite film-based resistive stain sensor that can be stretched up to 300% of strain value was introduced by Kurian et al. [6]. According to Kumar et al, conductive filler in polymer matrix can improve the mechanical and electrical properties of silicone-based sensors and actuators. He also presented the piezo-resistive strain sensor, which exhibits a tensile strength greater than 100% [7-8].

The entire system functions as a variable parallel plate film capacitor when DE is sandwiched between two compliant conducting electrodes, and its capacitance and resistance changes when it undergoes through variable stretching and relaxation cycles [9–11]. The base of DE-based strain sensor technology is variations in capacitance and resistance. Conducting films and textiles are the two main types of electrode are used in these kinds of sensors. Carbon powder, silver paint, metallic thin film, carbon grease, and carbon nanotubes hydrogel with electrolyte or graphene are some of the materials used to make conductive film-based electrodes [12–17].

Among these electrodes, carbon grease is generally widely utilized, due to high conductivity. Despite the widespread use of it, in many applications, carbon-based electrode doesn't retain conductivity at large strain and after numerous loading unloading cycles, cracks can also be developed. [18]. These types of sensors are difficult to fix in garments, which limits the use of carbon electrode-based sensors for wearable applications.

However, textile electrode-based sensors have good value of conductivity at large strain but fabric limits its elasticity. On the other hand, electrical measurement can produce good results in case of small sensing applications but at a higher value of strain, resistive sensors show nonlinear behavior because at large value of strain there are lot of factors can affect the resistance. [19-20]. To overcome these issues, in this work we are introducing stretchable capacitive strain sensor comprising of silicon elastomer and carbon nanotube based composite material as dielectric film and combination of fabric and liquid silicone as electrode.

In our fabrication process, electrodes are connected to the upper and lower side of dielectric film and additionally layer of liquid was used to adhere the electrodes on both side of dielectric film firmly. This liquid silicone makes the fabric more elastic and gives mechanical strength to the sensor. When sensor is stretched then this type of sensor provides more area for accumulation of charge consequently sensor's performance is improved.

Sensor performance mainly depend upon mechanical properties of sensor, nature of the electrode, selection of material. Currently this field is evolving and researchers are focusing on improving the performance of sensor in term of linearity and sensitivity of capacitive based sensors [21-23].

3.2 Experimental

3.2.1 Strain sensor fabrication

The strain sensor consists of an elastic dielectric film (length 65 mm, width 25 mm, film thickness 0.22 mm) squeezed between the upper and lower stretchable conducting fabric electrode layers(0.22mm) as shown in Fig. 1(a).

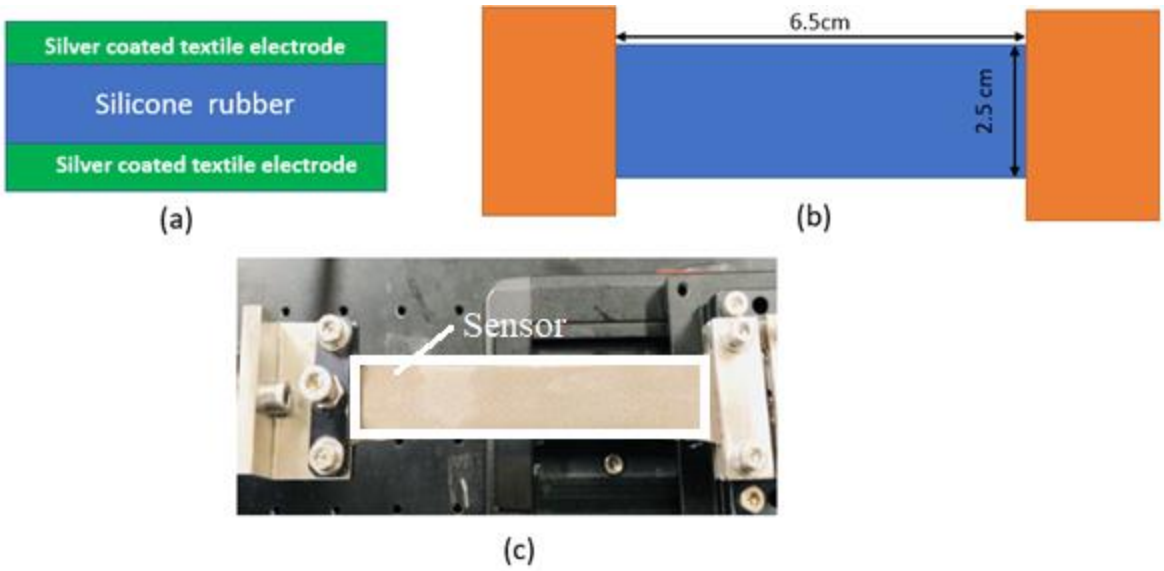

Fig. 1: (a) Schematic diagram of sensor structure (b) Dimension of the rectangular sensor specimen (c) Sensor fixed between two jaw of uniaxial tensile machine

The silicone elastomer based elastic film was prepared by solution casting from the two liquid silicone formulations (EcoflexTM 00-30, mixing part A & B equally by volume or weight) and further 0 .03 per hundred parts of rubber (phr) CNT was added in solution.

Silver coated fabric was used for electrodes. Liquid silicone layer was used on both side of dielectric film for adhering fabric electrodes on both sides.

Steps involved in fabrication process are explained in detail below:

- ✓ Mix Ecoflex 0030-part A and B equally by volume or weight.
- ✓ Add Single walled carbon nano tube (CNT), 0.03 parts per hundred rubber (phr) of CNT
- ✓ Stir CNT+ Ecoflex solution at 1500 rpm for 40 minutes with the help of magnetic stirrer
- ✓ Put solution in vacuum chamber for 30 minutes for degassing
- ✓ Pour solution on mould and leave it for 10 minutes at room temperature (make sure all air bubble has been removed) then put solution in oven for two hours at 90^0 C temperature.
- ✓ Let the film cooled down at room temperature after taking out of the oven
- ✓ To adhere the electrode on cured layer of dielectric film, an additional layer of Ecoflex (part A and B equal ratio) solution having 150µm thickness was caste on one side of fabric electrode later let fabric electrode leave at room temperature for 10 minutes so that silicone could fill the air gaps in fabric voids.

- ✓ Now again additional layer of Ecoflex (part A and B equal ratio) solution having 150µm thickness has been cast on cured dielectric film and put silicone mixed fabric electrode on top of it do the same process with another side of electrode and fabric and use roller for making thickness uniform and let it leave 10 minutes at room temperature after that put sensor in over for two hour at 90 degree and let it leave at room temperature for cooling. Now sensor is ready for use.

Formulation table is given below:

Table 1: Formulation table for fabricating Dielectric film

Material used for film fabrication	Mixing ratio		Stirring	Degassing	Curing time
	Ecoflex	CNT			
Ecoflex 00-30™ A & B	50:50	0.03phr	Stirred at 1500 rpm for 40 minutes	30 minutes in a vacuum chamber	two hours at 90^0C in oven
CNT					

3.3 Results and discussions

3.3.1 Electrical characterization of the Dielectric elastomer strain sensor (DSSS)

Dielectric elastomers belong to the electroactive polymer's family. DESS is made from three layers; one layer is made of dielectric material sandwiched by top and bottom layer of electrodes. This whole system is called variable parallel plate capacitor. On applying mechanical strain, geometry of this variable parallel plate capacitor changes which is lead to change in capacitance. After removal of mechanical strain, sensor again comes its original dimension. During stretching of DESS, length of the sensor increases while thickness decreases and both parameters overall lead to increase the capacitance of the sensor. On the other hand, when sensor comes its original position, length of sensor decreases and thickness increases and both parameters overall lead to decrease the value of capacitance and this change in capacitance can be utilized for various sensing mechanism.

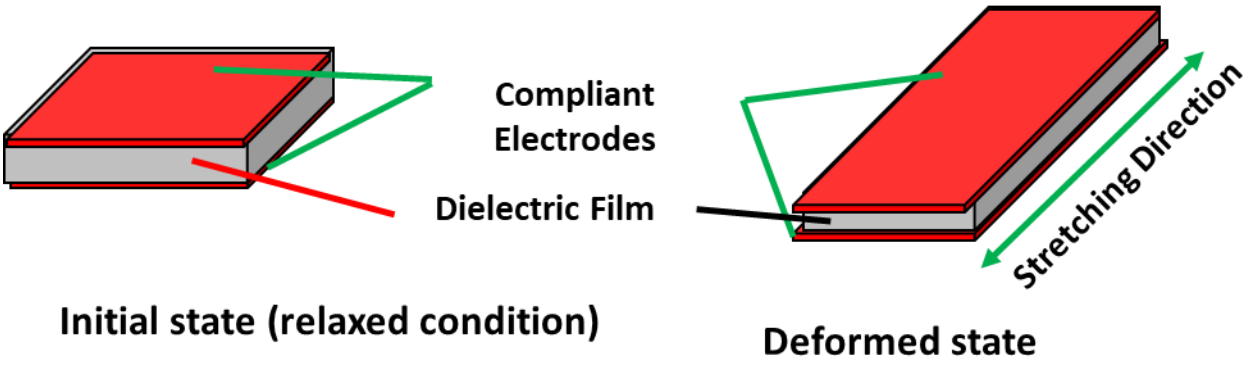

Fig. 2: Schematic representation of basic principle of DE strain sensor (DESS)

The capacitance of the DESS under a relaxed state ($C_{relaxed}$) can be written as:

$$C_{relaxed} = \frac{\varepsilon_r \varepsilon_0 L_1 L_2}{L_3} \qquad (1)$$

Where, L_1, L_2, L_3 are the length, width and thickness of the sensor in an un-deformed state. On the other hand, the Capacitance of a dielectric elastomer film capacitor in the stretched state can be written as:

$$C_{streched} = \frac{\varepsilon_r \varepsilon_0 \lambda_1 L_1 \lambda_2 L_2}{\lambda_3 L_3} \qquad (2)$$

Where, $\lambda_1, \lambda_2, \lambda_3$ are stretching ratio in the X, Y and Z direction respectively, while l_1, l_2 and l_3 are lengths, width and thickness in the deformed state, where: $\lambda_1 = \frac{l_1}{L_1}$, $\lambda_2 = \frac{l_2}{L_2}$, $\lambda_3 = \frac{l_3}{L_3}$.

When a DES sensor undergoes large deformation, the volumetric changes are often quite small as compared to the overall deformation. Therefore, volumetric deformation can be neglected, and assume that the material is incompressible, isotropic, and elastic. Considering a block of a DE material of the dimension with length width and thickness of the L_1, L_2 and L_3, respectively in the un-deformed state, is deformed up to the extent of l_1, l_2 and l_3, in the respective directions, and material is incompressible, the volume of the block must remain unchanged, namely, $L_1 L_2 L_3 = l_1 l_2 l_3$, or

$$\lambda_1 \lambda_2 \lambda_3 = 1 \qquad (3)$$

Consequently, we can write $l_3 = \frac{L_3}{\lambda_1 \lambda_2}$ (4)

$$C_{streched} = C_{relaxed}(\lambda_1 \lambda_2)^2 \quad (5)$$

In case of strain sensor undergoing uniaxial stretching upon applied external force, then $\lambda_1 = \lambda, \lambda_2 = \frac{1}{\sqrt{\lambda}} = \lambda_3$ consequently, we can write

$$C_{streched} = C_{\text{relaxed}} * \lambda \quad (6)$$

$$\Delta C = C_{\text{relaxed}} * \varepsilon \quad (7)$$

Where ε is strain, while, λ and ΔC are, extension coefficient and change in capacitance, respectively. The above equation depicts the linear change in the capacitance as a function of the extent of stretching.

For verifying analytic modeling of sensor with experimental values, capacitance of DESS was measured at multiple loading and unloading cycles at various value of strain, as shown in Fig. 3(b)

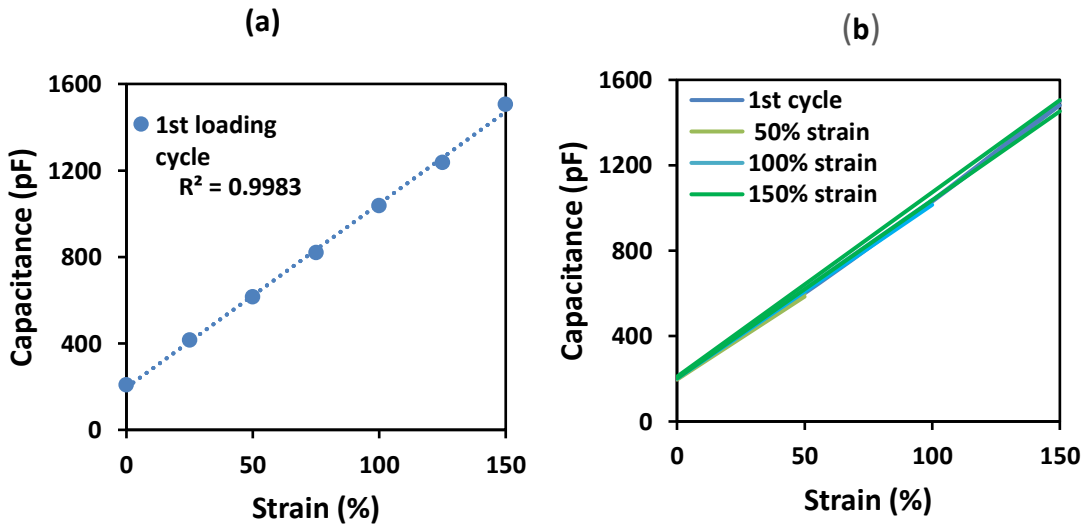

Fig. 3: (a) Capacitance and strain showing linear behaviour (b)Capacitance-strain characteristic of the DESS for the reversible multiple stretching and relaxation at different strain.

Fig.3 (a) shows that the capacitance increases linearly strain and Fig. 3(b) shows sensor is showing stable behavior after 1000 reversible relaxing and stretching cycles.

Capacitive sensor's performance is measured by sensitivity (gauge factor). Gauge factor of elastomer based capacitive sensor can be calculated by below mentioned formula

$$\text{Gauge factor (GF)} = \frac{C_s - C_r}{C_{r*\epsilon}} \quad (8)$$

In above equation *Cs* is capacitance at stretched state, *Cr* is capacitance at relaxed state and ϵ is strain. Gauge factor of each sample has been given below in Table 2

Table 2: Gauge factor of different specimen at different value of strain

Strain (%)	Gauge factor		
	After 1st loading cycling	After 1st unloading cycle	After 1000 cycles
50	4±0.06	4±0.08	4±0.08
100	4±0.08	4±0.09	4±0.09
150	4.1±0.09	4.1±0.08	4.1±0.09

Table 2 shows that even after 1000 stretching and unstretching cycles, the sensor's gauge factor value remains almost constant. Sensor is also showing comparatively good value of gauge factor t\and this kind of sensor is well suited for human activity monitoring and for different applications in wearables

3.3.1.1 Electrical characterization of conductive fabric

Knitted spandex fabric-based electrode coated with silver was used as an electrode, and silicone and CNT based composite film was used as a dielectric film. Conductivity of the electrode plays a crucial role in designing an effective capacitive sensing mechanism by demonstrating accommodating charges at various strain, which is responsible for capacitance variation. Additionally, conductivity should not vary with strain, so sheet resistivity of the fabric electrode was measured using a sheet resistivity meter. Fabric electrode was highly conductive even at large value of deformation. In Table 3 it can be clearly seen that resistivity of fabric electrode is very low (means highly conductive) and is almost constant at different strain levels.

Table 3: Sheet resistivity of fabric-based electrode at various value of strain values

Sheet resistivity (ohm/square)	Strain (%)
0.43	0
0.47	50
0.49	100
0.52	150

Sheet resistivity was almost constant (0.57 ohm/square) even after 1000 loading and unloading cycles at 150% value of strain.

Scanning electron microscope (SEM) analysis was also performed on fabric electrode for analyzing how silver coating disperse in fabric matrix at large deformation.

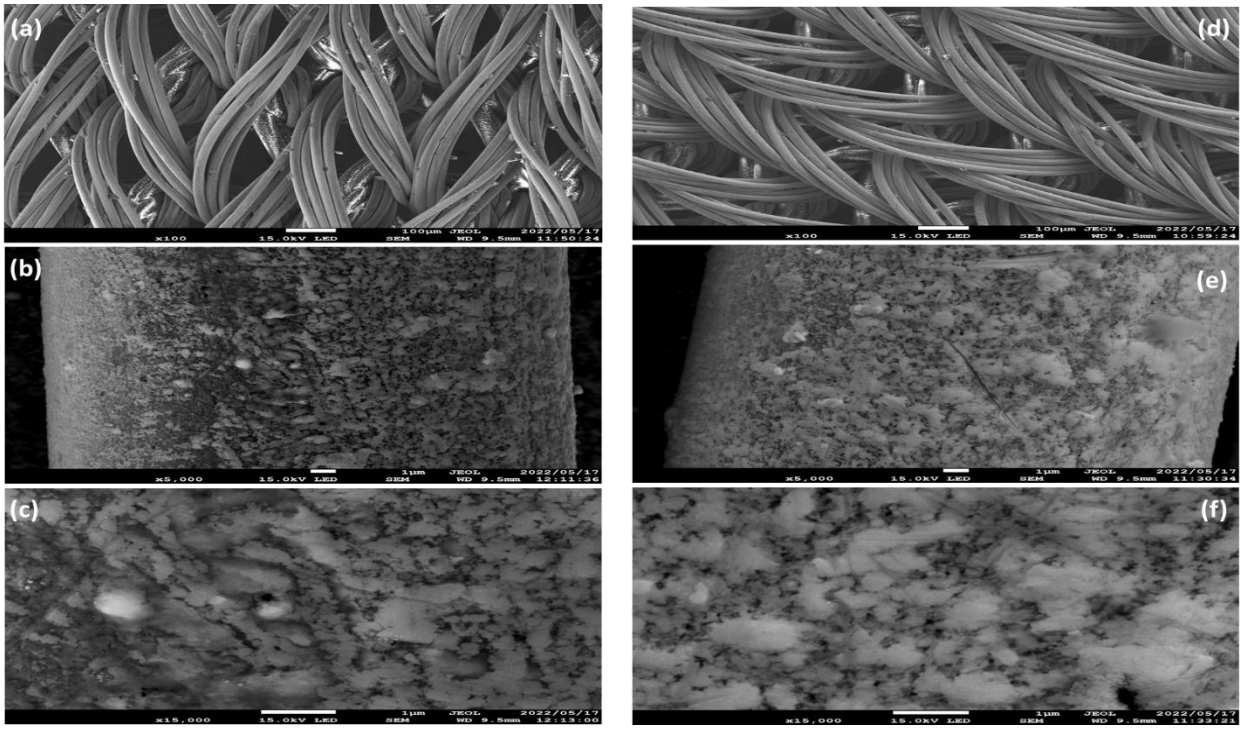

Fig. 4: (a), (b) and (c) are showing SEM analysis at 150% of strain value of fabric, single thread and macroscopic view of silver coating on single thread respectively. On the other hand, fig. (d), (e) and (f) are showing SEM analysis at relaxed state of fabric, single thread and silver coating on single thread respectively.

From Fig. 4, it can be concluded that quality of silver coating is not deteriorating with strain. It can be clearly seen that there is a uniform and continuous distribution of the silver layer even on a single thread of the fabric. Even at 150% elongation, the silver layer is clearly visible on the single yarn of the fabric and is uniformly distributed along the elongation direction, so the conductivity of the fabric is almost constant at different strain levels.

3.3.2 Mechanical characterization and modelling of the sensor

3.3.2.1 Uniaxial tensile measurement of the DES sensor

Although elastic DES sensors are generally considered incompressible and hyperelastic, but often exhibit inelastic behavior, especially at large strain. In fact, silicon rubber-based strain sensors, like any other strain sensor, can show stress relaxation behavior i.e stress can vary until few loading unloading cycles and it shows stable behavior after few cycles [24-28]. The Mullin effect is a temporary phenomenon that usually vanishes after a few loading unloading cycles (generally after 3 to 5 cycles). Mullins effect, can affect the cyclic stress-strain response of the sensor. This hysteresis response can be related to the viscosity of the material. Therefore, to understand this problem, uniaxial tensile testing was performed on sensor at different strain levels at strain rate of 10 mm/s. Fig. 5(a) shows the stress-strain curves for a DESS sensor during 5 loading and unloading cycles at different strain values ranging from 50% to 150%.

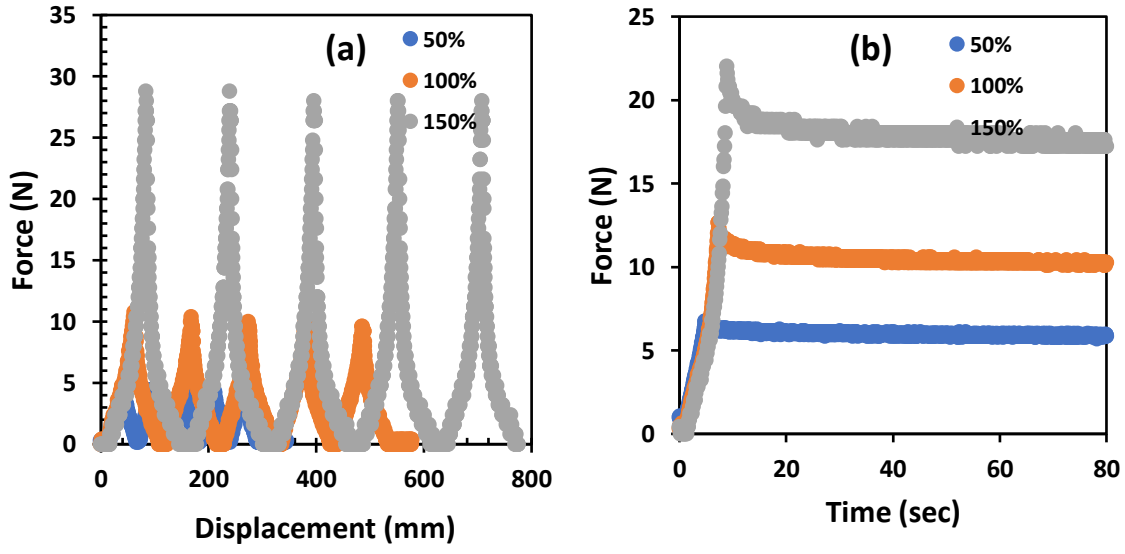

Fig. 5:(a) Force-strain curve of the DESS for the 5 loading unloading cycles (b) Time-dependent behaviour of sensor at different strain values. The initial length of the sensor was 65 mm.

In above figure length of sensor was 65 mm. From above figure it can be seen that force is almost constant in each cycle, concludes, Mullins effect can be neglected here.

In order to analyses the time-dependent behavior of sensor, DES sensor was held in the tensile machine at constant strain and from Fig. 5 (b) we can see that force is getting stabilized quickly until 100% of strain value and at 150% sensor is taking comparatively higher time in getting stabilized , consequently we can say that time dependent behaviour of sensor can be neglected until 100% of strain value but sensor is showing time dependent behaviour at 150% of strain value, which has been modeled later according to Prony series..

3.3.2.2 Uniaxial tensile measurement of the fabric electrode

For analyzing mechanical compatibility of fabric with silicone and CNT based dielectric film. Stress strain and time dependent behavior of fabric electrode and dielectric film was also analyzed individually at strain rate 10 mm/sec.

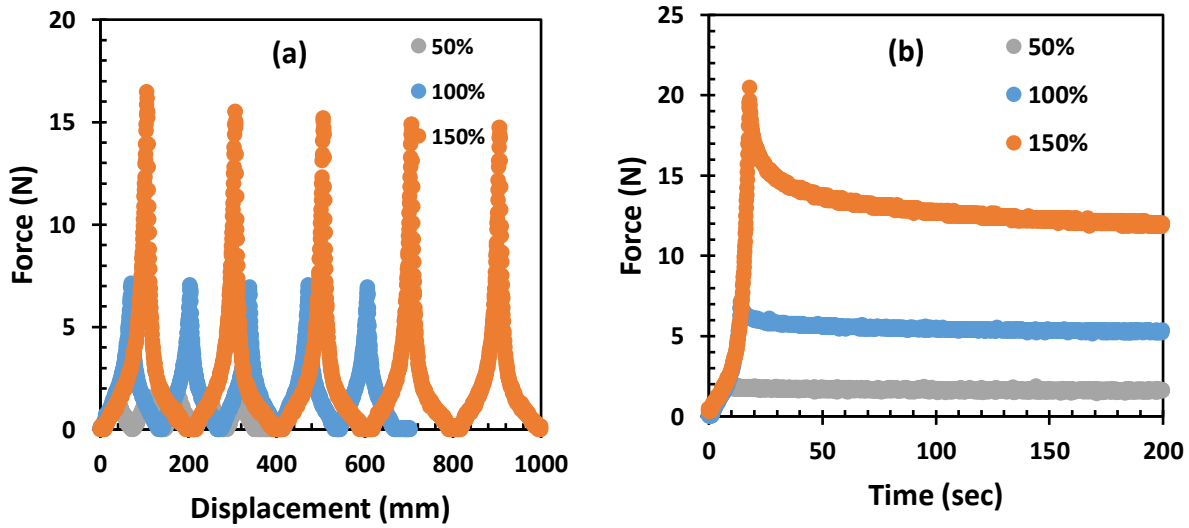

Fig. 6: (a) Force-displacement characteristics of fabric for 5 cycles (b) Time dependent behavior of fabric electrode at different strain values

In Fig. 6(a), the force-displacement analysis was performed on the fabric electrode at different elongation values for 5 cycles. From above graph, it can be concluded that fabric is not showing any considerable stress relaxation behavior until 100% value of strain. At 150% value of strain, stress relaxation behavior can be seen from Fig.6 (b). From above graph, it can be seen that the maximum force required to hold the sample stabilizes quickly at different strain values until 100% value of strain, but at 150% of strain value sensor is showing stress relaxation effect and stress is taking quite longer time in getting stabilized.

.

3.3.2.3 Uniaxial tensile measurement of the dielectric film

In Fig. 7(a) and (b) force displacement and time dependent behavior of composite film has been analyzed at strain rate 10mm/sec.

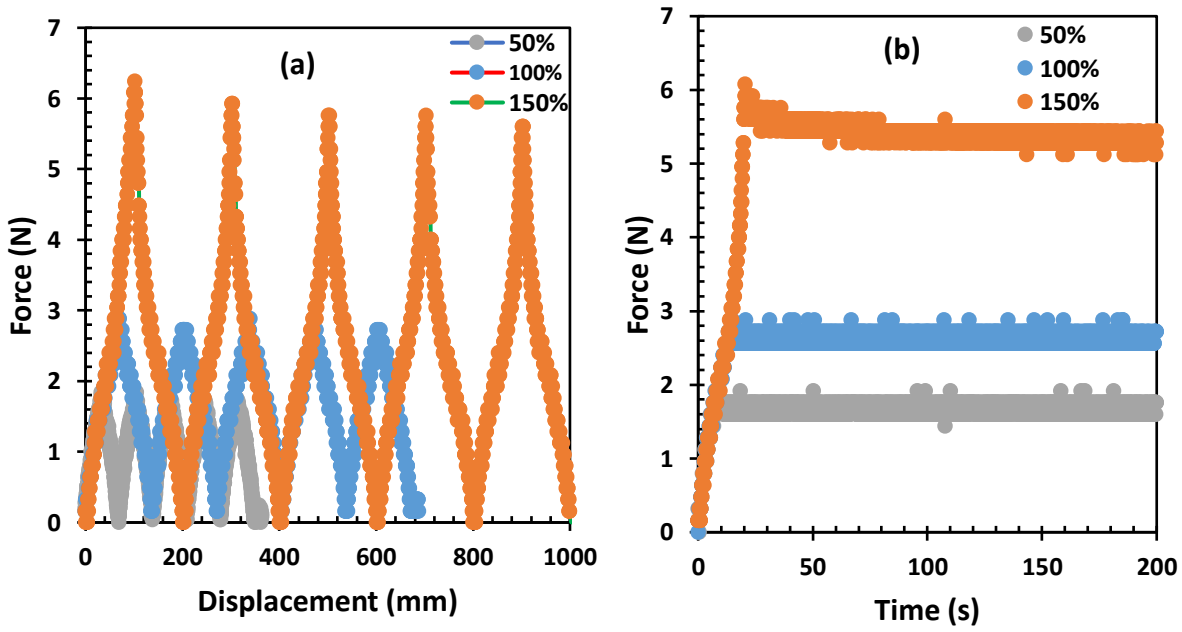

Fig. 7: (a) Force-displacement characteristics of dielectric film for 5 cycles (b) Time-dependent stress behaviour of the dielectric film at different strain

In Fig. 7 (a) Uniaxial tensile was run for five cycle at different strain levels and it can be clearly seen from the graph that force is constant in each cycle and graph is repetitive. Losses due to stress softening can be ignored. In Fig. 7(b) sample was held for 200 seconds at different strain levels to

observe that how much force is required to maintain that particular value of strain and it was concluded that force is becoming stable quickly shows material can be considered elastic and viscoelastic losses can be ignored.

From Fig. 6 and 7 it can be concluded that both dielectric film and fabric are following same trend at different value of strain and viscoelastic losses can be neglected until 100% value of strain in case of fabric electrode while in dielectric film viscoelastic losses were not observed even at 150 % value of deformation. consequently, it can be said that compatibility of sensor and fabric is very good even until 100% value of strain. We recommend use of this sensor until 100% value of strain.

3.3.3 Mechanical modelling of the DESS

The mechanical behaviour of the DES quite often does not follow Hook's law because of the nonlinear characteristic of the stress-strain curve, especially under large deformations. In continuum mechanics, nonlinear finite strain theory is utilized to explain huge deformations, as schematically shown in Fig. 8 [29].

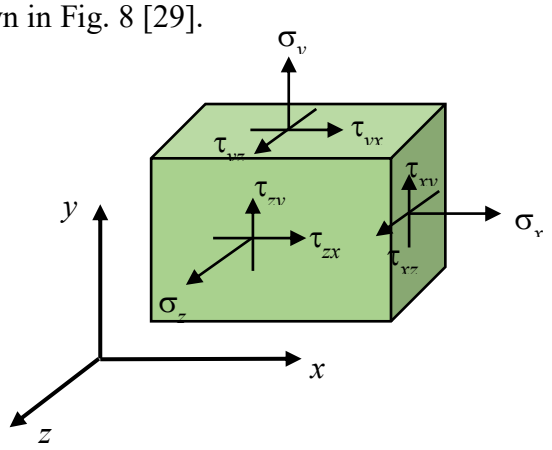

Fig. 8: The schematic diagram for description of nonlinear finite strain theory.

The constitutive model of a hyperelastic material assumes that the material is highly elastic, incompressible, and isotropic, where the time-dependent mechanical response can be ignored. μ_i and α_i are material parameters. For an incompressible, isotropic material, the true stress T_i can be given by the derivative of the strain energy potential *(W)* with respect to the stretch ratio λ_i

$$T_i = \lambda_i \frac{\partial W}{\partial \lambda_i} - p \qquad (9)$$

Normal stress linked to the stretch ratio λ_i can be estimated by dividing the above equation by a factor λ_i, where p is hydrostatic pressure.

$$\sigma_i = \frac{\partial W}{\partial \lambda_i} - \frac{1}{\lambda_i} p \qquad (10)$$

The nine components of σ_{ij} as shown in Fig. 8 (normal stress vectors) are the components of a second-order Cartesian tensor, which can define stress at a point and is given by the following equation.

$$\sigma_{ij} = \begin{pmatrix} \sigma_x & \sigma_{xy} & \sigma_{xz} \\ \sigma_{yx} & \sigma_y & \sigma_{yz} \\ \sigma_{zx} & \sigma_{zy} & \sigma_z \end{pmatrix} \qquad (11)$$

Above matrix can be written alternately as following equation, where off diagonal elements are the shear terms.

$$\sigma_{ij} = \begin{bmatrix} \sigma_x & \tau_{xy} & \tau_{xz} \\ \tau_{yx} & \sigma_y & \tau_{yz} \\ \tau_{zx} & \tau_{zy} & \sigma_z \end{bmatrix} \qquad (12)$$

The components σ_{ij} of the stress, tensor depends on the orientation of the coordinate system at the point under consideration. In above equation τ is shear term.

3.3.3.1 Principal stresses and directions

At any point on the loaded or stressed body, at least 3 planes called principal planes exist, with normal vector n, called principal directions. Where, the corresponding stress vector is normal to the plane. This has been schematically shown in Fig.9. In the absence of normal shear stress τ_n, these three stresses perpendicular to these principal planes are called principal stresses.

$$\sigma_{ij} = \begin{pmatrix} \sigma_x & 0 & 0 \\ 0 & \sigma_y & 0 \\ 0 & 0 & \sigma_z \end{pmatrix} \qquad (13)$$

The principal planes are devoid of stress, but the principal axes are the only directions in which stress can be experienced. The directions of the principal axes are orthogonal to the directions of the principal planes. According to the Cauchy's Theorem:

$$T_i = \sigma_{ij} n_i \qquad (14)$$

Where T_i is the true stress vector at a point on a plane with normal vector n_i

Ti is symmetric and represents the pressure (force per unit area acting on a section) of the deformed body across a plane with an outer normal vector n. The principal stresses σ_x,$\sigma_y$and σ_z, are the roots of the characteristic equation. A principle direction n_1, n_2 and n_3 corresponds to each principal stress and can be utilized to build a principal coordinate system. Every tensor has certain invariants that are independent of the coordinate system, such as the magnitudes of the normal stress vectors or primary stresses, which correspond to the constant of proportionality λ. In this particular case, λ is corresponded to the magnitude of normal stress vector (σ_n) or principal stress magnitude.

$$T_i = \lambda n_i = \sigma_{ji} n_i \qquad (15)$$

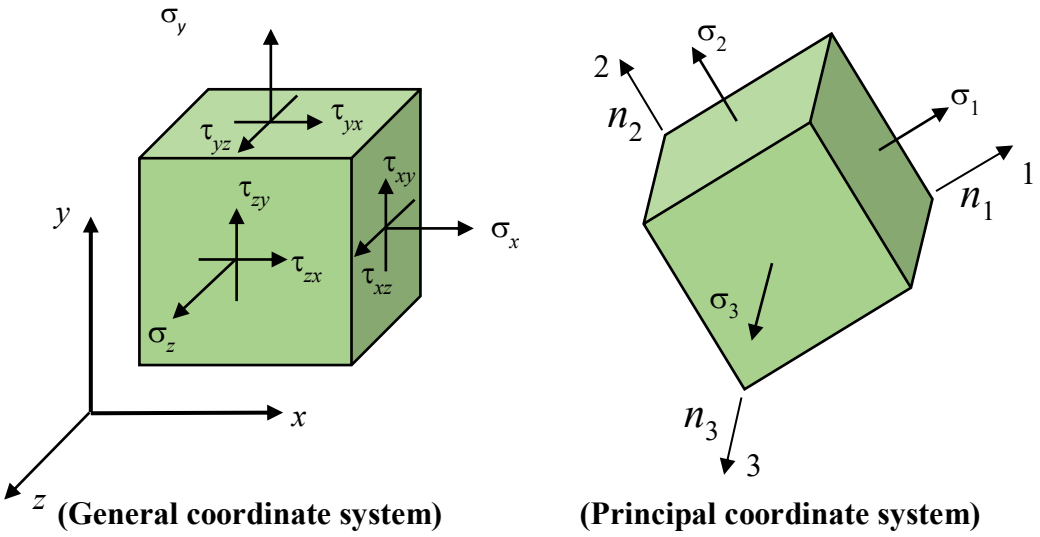

Fig. 9: The schematic diagram for describing principal stresses and directions

This is for a homogeneous system of 3 linear equations, where n_i are the unknowns . The determinant matrix of the coefficients must be equal to zero for getting a nontrivial solution. Therefore,

$$\begin{aligned}(\sigma_x-\lambda)n_1+\tau_{xy}n_2+\tau_{xz}n_2=0\\ \tau_{xy}n_1+(\sigma_y-\lambda)n_2+\tau_{yz}n_3=0\\ \tau_{xz}n_1+\tau_{yz}n_2+(\sigma_z-\lambda)n_3=0\end{aligned}\Rightarrow\begin{bmatrix}(\sigma_x-\lambda) & \tau_{xy} & \tau_{xz}\\ \tau_{xy} & (\sigma_y-\lambda) & \tau_{yz}\\ \tau_{xz} & \tau_{yz} & (\sigma_z-\lambda)\end{bmatrix}\begin{bmatrix}n_1\\ n_2\\ n_3\end{bmatrix}=0 \qquad (16)$$

$$\begin{vmatrix}(\sigma_x-\lambda) & \tau_{xy} & \tau_{xz}\\ \tau_{xy} & (\sigma_y-\lambda) & \tau_{yz}\\ \tau_{xz} & \tau_{yz} & (\sigma_z-\lambda)\end{vmatrix}=0\Rightarrow -\lambda^3+I_1\lambda^2-I_2\lambda+I_3=0 \qquad (17)$$

The homogeneous system of algebraic equations has a non-trivial solution, and expanding determinant gives characteristic equation having three real roots λ means these roots are not imaginary because of the symmetry of the stress tensor. The Cayley–Hamilton theorem's roots are the eigenvalues. For every stress tensor, the primary stresses are unique. Therefore, from the above equation, the coefficients I_1, I_2 and I_3, called the 1st, 2nd and 3rd stress invariants respectively, have always identical value.

$$I_1=Tr|\sigma_{ij}| \qquad (18)$$

$$I_2=\tfrac{1}{2}\left[Tr(\sigma_{ij})^2-Tr(\sigma_{ij}{}^2)\right] \qquad (19)$$

$$I_3=det(\sigma_{ij})=1 \qquad (20)$$

3.3.4 Time independent constitutive modelling of Dielectric elastomer strain sensor (DESS)

3.3.4.1 Constitutive modelling of the sensor

The mechanical behaviour of hyperplastic materials can be explained by the strain energy function W, which depends on strain variants I_1 and I_2, can be derived from the below expressions: The left or right Cauchy-Green deformation tensor can be given by

$$\boldsymbol{B} = \boldsymbol{F}\boldsymbol{F}^T \Rightarrow Left\ \ Cauchy - Green\ deformation\ tensor \text{ ------- (21)}$$
$$\boldsymbol{C} = \boldsymbol{F}^T\boldsymbol{F} \Rightarrow\ Right\ Cauchy - Green\ deformation\ tensor \text{ ------ (22)}$$

Where, B, C and F are, left Cauchy, right Cauchy and deformation tensor, respectively. F can be denoted by

$$\boldsymbol{F} = \begin{bmatrix} \frac{\partial x_1}{\partial X_1} & \frac{\partial x_1}{\partial X_2} & \frac{\partial x_1}{\partial X_3} \\ \frac{\partial x_2}{\partial X_1} & \frac{\partial x_2}{\partial X_2} & \frac{\partial x_2}{\partial X_3} \\ \frac{\partial x_3}{\partial X_1} & \frac{\partial x_3}{\partial X_2} & \frac{\partial x_3}{\partial X_3} \end{bmatrix} = \begin{bmatrix} \lambda_1 & 0 & 0 \\ 0 & \lambda_2 & 0 \\ 0 & 0 & \lambda_3 \end{bmatrix} \quad (23)$$

$$I_1 = \lambda_1^2 + \lambda_2^2 + \lambda_3^2 \quad (24)$$
$$I_2 = \lambda_1^2\lambda_2^2 + \lambda_2^2\lambda_3^2 + \lambda_3^2\lambda_1^2 \quad (25)$$

In the above equations, we can also write *C* instead of *B*. I_1 and I_2 can be calculated from principal stretch ratios λ_i (i = 1, 2 and 3). Polynomial strain energy function can be written as a phenomenological model based on the 1st and 2nd strain invariants I_1 and I_2, as mentioned below[30]:

$$W_{Polynomial\ form} = \sum_{i+j=1}^{N} C_{ij}\,(I_1 - 3)^i (I_2 - 3)^j + \sum_{k=1}^{N} \frac{1}{D_k}(J-1)^{2k} \quad (26)$$

In the above equation, Cij, N, J, and D_k are the material constants, number of terms, volumetric coefficient, and material incompressibility parameters respectively. The initial shear (μ_0) is 2 (C_{10}+C_{01}) and the bulk moduli is 2/D1. Material constants such as C_{ij} and D_k describe nonlinear mechanical behavior and are essential for designing of engineering components made of

elastomeric materials. With the help of these material sensor's behaviour can be predicted under all types of loads (uniaxial to multiaxial). The constants Cij and Dk can be determined from experimental stress-strain curves using the curve fitting. For hyperelastic modeling, the material can be assumed to be completely or nearly incompressible, isotropic, and elastic. Therefore, in case of hyperelastic modeling J can be assumed 1 in above equation. This is the basic equation adopted in several models with some changes to describe the material properties of a rubbery materials.

3.3.4.1.1 Mooney-Rivlin model

A hyperelastic isotropic material model called Mooney-Rivlin model was developed by Mooney-Rivlin to explain the stress-strain characteristics of rubber-like materials [31]. Generally, Mooney-Rivlin models is used to model the nonlinear behavior of incompressible materials. By putting N=1 in eq. (26) first order of this model, can be written as,

$$W_{Mooney-Rivlin} = C_{10}(I_1 - 3) + C_{01}(I_2 - 3) \qquad (27)$$

In this model mechanical energy is denoted by the sum of invariants.

3.3.4.1.2 Yeoh model

Yeoh model proposed by a cubic form having only 1st invariant I_1, applicable on incompressible materials, where C_{i0} are material constants [32]. Yeoh model solely depend upon first invariant I_1.

$$W_{Yeoh} = \sum_{i=1}^{N} C_{i0}\,(I_1 - 3)^i \quad \text{---------- (28)}$$

This model is ok for small and simple data but for big and complex data sometimes this mode does not work well.

3.3.4.1.3 Neo-Hookean model

The Neo-Hookean model is a subset of polynomial form for N=1, C_{01}=0, and C_{10}=μ/2 [33]

$$W_{Neo-Hookean} = \frac{\mu}{2}(I_1 - 3) \qquad (29)$$

Although Neo-Hookean model is simple but at large strain sometimes it does not give good results.

3.3.4.1.4 Ogden model

The Ogden form can be denoted as a function of the principal stretch ratios:

$$W_{Ogden} = \sum_{i=1}^{N} \frac{\mu_i}{\alpha_i} (\lambda_1{}^{-\alpha_i} + \lambda_2{}^{-\alpha_i} + \lambda_3{}^{-\alpha_i} - 3) \qquad (30)$$

Where μ_i and α_i are material constants. It is desirable to calculate these material constants for predicting and analysing mechanical behaviour of sensor at different strain values in multi axial loadings. Due to based on principal stretch ratios, Ogden model gives comparatively better results even at large value of strain. However, in case of small dataset this model does not show good fitting results.

In above constitutive equations initial shear modulus for Yeoh, Ogden, Mooney-Rivlin and Neo-Hookean model can be obtained by 2 C_{10}, 0.5(μ_1* α_1), 2(C_{10}+ C_{01}), 2 C_{10} respectively.

Table 4: Strain vector at in case of uniaxial, Biaxial, pure shear

Type of loading	Uniaxial	Biaxial	Pure shear
Strain vector	$\begin{bmatrix} \lambda & 0 & 0 \\ 0 & \frac{1}{\sqrt{\lambda}} & 0 \\ 0 & 0 & \frac{1}{\sqrt{\lambda}} \end{bmatrix}$	$\begin{bmatrix} \lambda & 0 & 0 \\ 0 & \lambda & 0 \\ 0 & 0 & \frac{1}{\lambda^2} \end{bmatrix}$	$\begin{bmatrix} \lambda & 0 & 0 \\ 0 & 1 & 0 \\ 0 & 0 & \frac{1}{\lambda} \end{bmatrix}$
Invariants I_1 & I_2	$I_1 = \lambda^2 + \frac{2}{\lambda}$ $I_2 = 2\lambda + \frac{1}{\lambda^2}$	$I_1 = 2\lambda^2 + \frac{1}{\lambda^4}$ $I_2 = \lambda^4 + \frac{2}{\lambda^2}$	$I_1 = I_2 = 1 + \lambda^2 + \frac{1}{\lambda^2}$

Uniaxial tensile testing was performed on DESS sensor at 100% of strain value and obtained data was used for 3 cycles at strain rate of 1mm/sec as shown in Fig. 10 (left).

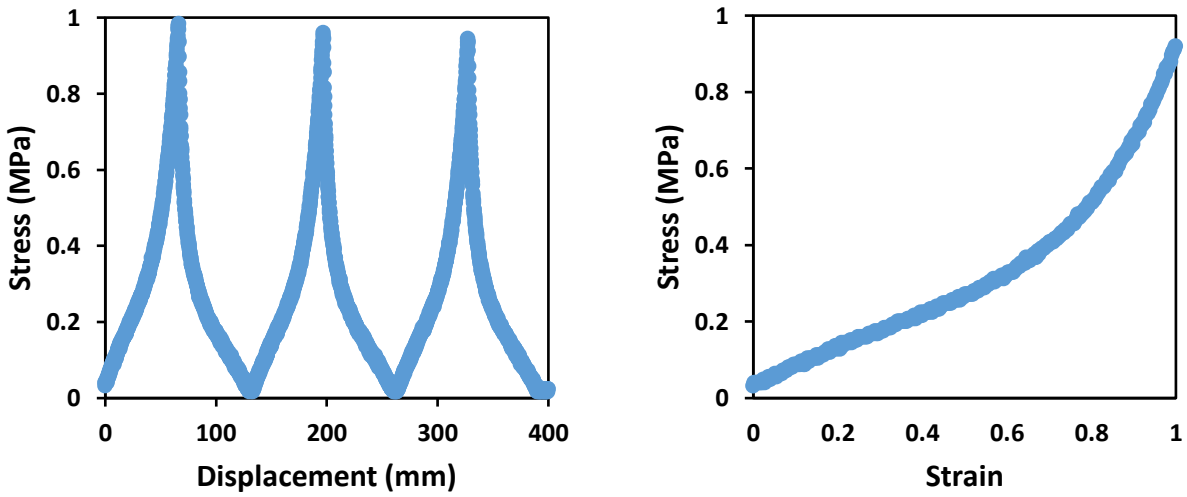

Fig. 10: Strain-strain characteristics for 3 cycles (left) and first half loading cycle at 100% strain value (right) for the DE sensor having initial length 65 mm

Fig. 10 shows that sensor is showing stable behavior as maximum stress is almost same in all three cycles so we can consider that this sensor is showing hyperpelastic behavior until 100% of strain value and viscoelastic losses are small which can be neglected. For post processing of data, first half loading cycle's data was chosen and further it was fitted with first term of different constituting modeling equations. It was found that Ogden first term's model is close to the experimental data, so in next step Ogden second term was used to fit the experimental data and it was found that Ogden second term was well fit with experimental data. Later experimental data was also fitted Ogden 3rd term and it was also fitted with experimental data so it was concluded that experimental data starts fitting with 2nd term (fitting increase on increasing order of term) of Ogden model and from 2nd Ogden term any term's fitting parameters can be used for modeling the stress strain behavior of sensor at different strain value and can use fitting parameters for predicting sensor behavior in different multiaxial loading at any strain value, which is very useful in designing a sensor and can save researchers time in doing several experiments.

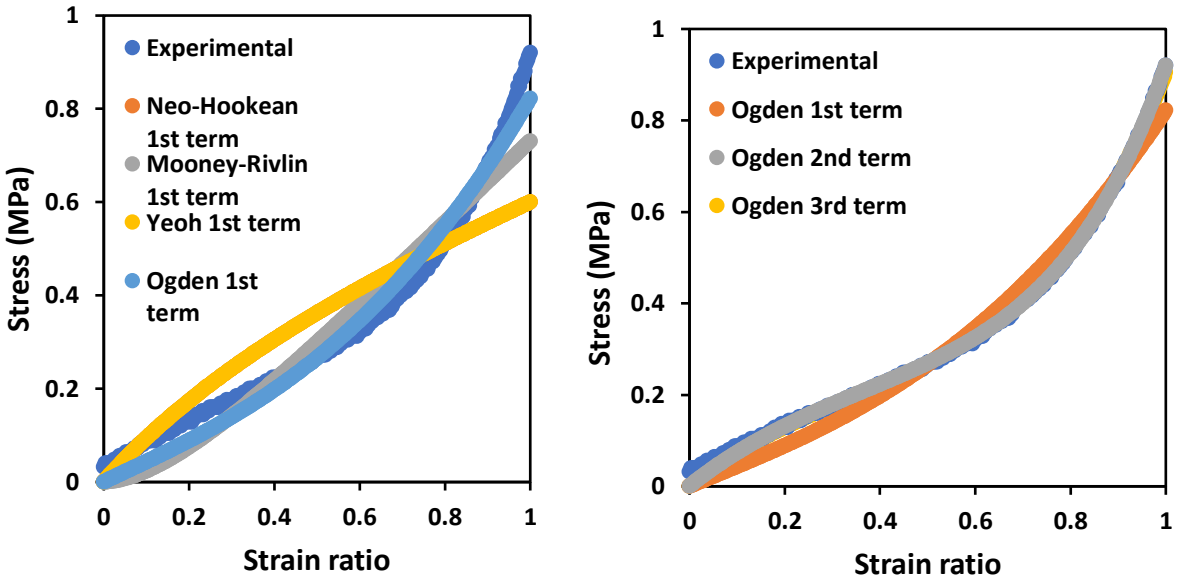

Fig. 11: Different theoretical modeling on first loading cycle (left) fitting of experimental data upto 3rd term of Ogden (initial length 65 mm)

Different fitting parameters were obtained from various constitutive modeling, as summarized in Table 5 can be used for predicting and analyzing sensor behavior in different types of loading.

Table 5: fitting parameters obtained from the fitting of the experimental data using different theoretical constitutive models.

Constants	Yeoh ($_1$st term)	Ogden terms			Mooney-Rivlin ($_1^{st}$ term)	Neo-Hookean ($_1^{st}$ term)
		$_1^{st}$ term	$_2^{nd}$ term	$_3^{rd}$ term		
C_{10} (MPa)	0.17(±.01)	NA	NA	NA	0.41 (±0.03)	NA
C_{01} (MPa)	NA	NA	NA	NA	-0.40 ± (0.04)	NA
μ (MPa)	NA	0.14(±0.003)	0.005 (±0.0003), 0.27 (±.31)	0.018 (±0.0004), -1.23 (±0.04), 1.53 (±0.05)	NA	0.34(±0.04)
α (MPa)	NA	4.78 (±.06)	10.25 (± 0.48), 0.01 (±0.04)	8.52 (±0.64), 0.58 (±0.06), -0.014 (±0.004)	NA	NA

$$\text{Uniaxial} = \sigma_{Odgen} = \sum_{i=1}^{N} \mu_i \left(\lambda^{\alpha_i} - \lambda^{-\alpha_{i/2}}\right) \qquad (31)$$

$$\text{Biaxial} = \sigma_{Odgen} = \sum_{i=1}^{N} \mu_i \left(\lambda^{\alpha_i} - \lambda^{-2\alpha_i}\right) \qquad (32)$$

$$\text{Pure shear} = \sigma_{Odgen} = \sum_{i=1}^{N} \mu_i \left(\lambda^{\alpha_i} - \lambda^{-\alpha_i}\right) \qquad (33)$$

From above Table 5, After calculating μ_i and α_i and and putting both constant values in eq. (31), sensor mechanical characteristics can be predicted at any value of deformation, similarly, we can use these constants can also be used for predicting sensor behaviour in other types of loading like biaxial, pure shear etc

3.3.5 Time dependent constitutive model of DESS

At 150% of the strain value, the sensor exhibits time dependent behaviour. It can be seen from Fig. 6 (b) that when holding a constant strain at 150% of the voltage, the force required to maintain that strain takes slightly longer to establish (compared to a 100% voltage). The equation below can be used to explain the sensor's time-dependent stress relaxation behavior:

$$\sigma(t) = R(t)\varepsilon \tag{34}$$

Where $\sigma(t)$ is time dependent stress, $R(t)$ is stress relaxation function and ε is initial strain. Strain relaxation function $R(t)$ can be modeled by using Prony series, as given below [34]:

$$R(t) = R_{ins}[1 - \sum_{i=1}^{n} P_i\,(1 - e^{-t/\tau_i})] \tag{35}$$

Where R_{ins} is instantaneous value of stress relaxation function, P_i is *i'th* Prony term and τ_i is *i'th* Prony relaxation time and t is the time.

Fig. 12 shows time dependent behaviour of sensor at strain =150%. Stress vs time data was fitted according to Prony series and it was found that stress vs time graph was well fit with 4th order of Prony series and fitting parameters were calculated, as given in in the table 7.

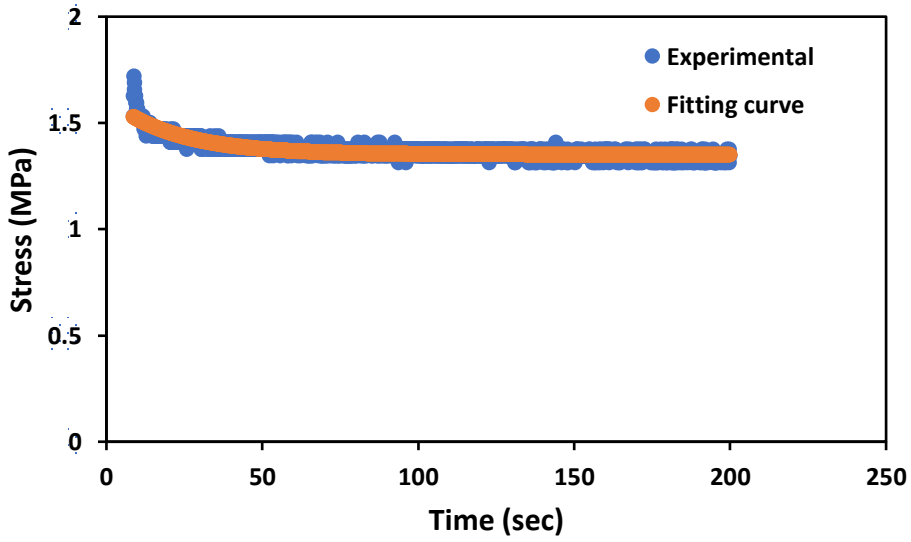

Fig. 12. Fitting of the experimental data using Prony series-based relaxation function.

This Prony series based viscoelastic model can be used to analyze sensor behaviour at any value of time and stress can be easily predicted by suing this model.

Table 6: Parameters for the DE sensor extracted after fitting the experimental data by 4^{th} order Prony series.

Fitting parameters	Estimated values
R_{ins}	2.84
P_1	0.18
τ_1	3.62
P_2	0.31
τ_2	4.94
P_3	0.03
τ_3	99.27
P_4	0
τ_4	29.71

The time-dependent behavior of the sensor can be predicted for any value of time after putting these fitting parameters in above equation.

3.4 Conclusions

Dielectric elastomer-based strain sensors were fabricating using combination of silicone rubber and CNT as composite dielectric film and combination of liquid silicone and silver coated fabric was used as an electrode. Sensor was showing stable behavior even after 1000 loading and unloading cycles and fabric electrode was not losing its conductivity even at large value of strain. Electromechanical modeling of sensor was explained in 3D space and further this numerical modeling was also validated using experimental data. Gauge factor was also calculated and sensor was showing comparatively better value of gauge factor. Mechanical characterization of sensor was conducted by using uniaxial tensile testing at different strain values. Further time dependent and time independent behavior of sensor was modeled using different theoretical modeling and fitting parameters were obtained for predicting sensor behaviour at different strain values and in different types of loading conditions which is every important for designing a sensor.

3.5 References

[1] M. Amjadi, K.U. Kyung, I. Park, and M. Sitti, Stretchable, skin-mountable, and wearable strain sensors and their potential applications: A review, Advanced Functional Materials, vol.26, no.11, pp. 1678–1698, (2016).

[2] G. D. Panozzo, O. Hilliges, and O. Sorkine-Hornung, Deformation capture via soft and stretchable sensor arrays, ACM Transactions on Graphics, vol. 38, no. 2, pp. 1–16, (2019).

[3] A Qiu, Q Jia., H Yu., J. A. Oh, D Li., H. Y. hsu, and J. Ma. Highly sensitive and flexible capacitive elastomeric sensors for compressive strain measurements. Materials Today Communications, 26, 102023(2021).

[4] N. K. Singh, K. Takashima, and S. S. Pandey, "Fatigue life prediction of electroactive polymer strain sensor," Electroactive Polymer Actuators and Devices (EAPAD) XXIII, Online Only, United States, (2021).

[5] T Wang., M. Farajollahi, Y.S. Choi, I. T. Lin, J. E Marshall, and S. K. Smoukov, (2016). Electroactive polymers for sensing. Interface focus, 6(4), 20160026.

[6] A. S. Kurian, V. B. Mohan, and D. Bhattacharyya, Embedded large strain sensors with graphene-carbon black-silicone rubber composites, Sensors and Actuators A: Physical, vol. 282, pp. 206–214, Oct. 2018.

[7] V. Kumar, G. Lee, Monika, J. Choi, and D.-J. Lee, Studies on composites based on HTV and RTV silicone rubber and carbon nanotubes for sensors and actuators, Polymer, vol. 190, p. 122221, Mar. 2020.

[8] V. Kumar, G. Lee, K. Singh, J. Choi, and D.-J. Lee, Structure-property relationship in silicone rubber nanocomposites reinforced with carbon nanomaterials for sensors and actuators, Sensors and Actuators A: Physical, vol. 303, p. 111712, Mar. 2020

[9] N. K. Singh, K. Takashima, and S. S. Pandey, Tear strength estimation of electroactive polymer-based strain sensors, in Electroactive Polymer Actuators and Devices (EAPAD) XXIV, Eds. Long Beach, United States, Mar. 6–Apr. 11, 2022. SPIE, 2022.

[10] T Wang., M. Farajollahi, Y.S. Choi, I. T. Lin, J. E Marshall, and S. K. Smoukov, (2016). Electroactive polymers for sensing. Interface focus, 6(4), 20160026.

[11] K. Ozlem, O. Atalay, A. Atalay, and G. Ince, Textile based sensing system for lower limb motion monitoring, in Converging Clinical and Engineering Research on Neurorehabilitation III. Cham: Springer International Publishing, (2018), pp. 395–399.

[12] L.Beccai, C. Lucarotti, M. Totaro, and M. Taghavi, Soft robotics mechanosensing, in Soft Robotics: Trends, Applications and Challenges. Cham: Springer International Publishing, (2016), pp. 11–21.

[13] Y.-D. Tao, G.-Y. Gu, and L.-M. Zhu, Design and performance testing of a dielectric elastomer strain sensor, International Journal of Intelligent Robotics and Applications, vol. 1, no. 4, pp. 451–458, (2017).

[14] H. Zhang, M. Y. Wang, J. Li, and J. Zhu, A soft compressive sensor using dielectric elastomers, Smart Materials and Structures, vol. 25, no. 3, p. 035045, (2016)

[15] T. Dong, Y. Gu, T. Liu, and M. Pecht, Resistive and capacitive strain sensors based on customized compliant electrode: Comparison and their wearable applications, Sensors and Actuators A: Physical, vol. 326, p. 112720, (2021).

[16] Atalay, Textile-Based, interdigital, capacitive, soft-strain sensor for wearable applications, Materials, vol. 11, no. 5, p. 768, (2018).

[17] J.-w. Zhang, Y. Zhang, Y.-y. Li, and P. Wang, Textile-Based flexible pressure sensors: A review, Polymer Reviews, pp. 1–31, (2021).

[18] C. A. de Saint-Aubin, S. Rosset, S. Schlatter, and H. Shea, High-cycle electromechanical aging of dielectric elastomer actuators with carbon-based electrodes, Smart Materials and Structures, vol. 27, no. 7, p. 074002, (2018)

[19] S. Rosset and H. R. Shea, Flexible and stretchable electrodes for dielectric elastomer actuators, Applied Physics A, vol. 110, no. 2, pp. 281–307, (2012)

[20] K. Jung, K. J. Kim, and H. R. Choi, A self-sensing dielectric elastomer actuator, Sensors and Actuators A: Physical, vol. 143, no. 2, pp. 343–351, (2008).

[21] L. A. Toth and A. A. Goldenberg, Control system design for a dielectric elastomer actuator: The sensory subsystem, in SPIE's 9th Annual International Symposium on Smart Structures and Materials, Y. Bar-Cohen, Ed. San Diego, CA. SPIE, (2002).

[22] M. Wissler and E. Mazza, Mechanical behavior of an acrylic elastomer used in dielectric elastomer actuators, Sensors and Actuators A: Physical, vol. 134, no. 2, pp. 494–504, (2007).

[23] N. K. Singh, K. Takashima, and T. Shibata, "Dielectric elastomer based stretchable textile sensor for capturing motion," in Electroactive Polymer Actuators and Devices (EAPAD) XXII, Eds. Online Only, United States, Apr. 27–May 8, 2020. SPIE, 2020.

[24] X. Liu et al., Dielectric elastomer sensor with high dielectric constant and capacitive strain sensing properties by designing polar-nonpolar fluorosilicone multiblock copolymers and introducing poly(dopamine) modified CNTs, Composites Part B: Engineering, vol. 223, p. 109103, (2021)

[25] M. Kollosche, H. Stoyanov, S. Laflamme, and G. Kofod, Strongly enhanced sensitivity in elastic capacitive strain sensors, Journal of Materials Chemistry, vol. 21, no. 23, p. 8292, (2011)

[26] H. Stoyanov, M. Kollosche, D. N. McCarthy, and G. Kofod, Molecular composites with enhanced energy density for electroactive polymers, Journal of Materials Chemistry, vol. 20, no. 35, p. 7558, (2010).

[27] Z. Suo, Theory of dielectric elastomers, Acta Mechanica Solida Sinica, vol. 23, no. 6, pp. 549–578, (2010).

[28] X. Lv, L. Liu, Y. Liu, and J. Leng, Electromechanical Modeling of Softening Behavior for Dielectric Elastomers, Journal of Applied Mechanics, vol. 85, no. (2018).

[29] X. Chen, Q.Tan,h liang Introduction to mechanical metamaterials and their effective properties, Comptes Rendus. Physique, pp. 1–15, Nov. (2020)

[30] Khajehsaeid, H., J. Arghavani, and R30311651347 Naghdabadi. "A hyperelastic constitutive model for rubber-like materials." European Journal of Mechanics-A/Solids 38 (2013): 144-151.

[31] Y. Bai, C. Liu, G. Huang, W. Li, and S. Feng, A hyper-viscoelastic constitutive model for polyurea under uniaxial compressive loading, Polymers, vol. 8, no. 4, p. 133, (2016)

[32] S. D. Barforooshi and A. K. Mohammadi, Study Neo-Hookean and Yeoh Hyper-Elastic Models in Dielectric Elastomer-Based Micro-Beam Resonators, Latin American Journal of Solids and Structures, vol. 13, no. 10, pp. 1823–1837, (2016).

[33] A. Abdelsalam, S. Araby, M. A. Hassan, and A. A. El-Moneim, Constitutive modelling of elastomer/graphene platelet nanocomposites, IOP Conference Series: Materials Science and Engineering, vol. 244, p. 012016, (2017).

[34] Hristov, Jordan Yankov. "Linear viscoelastic responses: The Prony decomposition naturally leads into the Caputo-Fabrizio fractional operator." *Frontiers in Physics* 6 (2018): 135.

CHAPTER-4

IONIC ELECTROACTIVE POLYMER-BASED STRAIN SENSOR

4.1 Introduction

Ionic EAP typically operates at low voltages (less than 5 V) which makes them perfect for sensing and actuation applications. Materials used for the synthesis of Ionic EAPs such as polypyrrole (PPy) and poly (3,4 ethylenedioxythiophene) (PEDOT) are generally biocompatible. Therefore, such EAPs are suitable for biological applications too.

Ionic EAP usually requires an ion reservoir to transport ions or molecules within it. Due to the presence of ions, these types of EAPs show some common characteristics like responsive material, strain or the stress applied to these materials causes ions migration, and charge distribution. Properties of ion transportation are responsible for sensing phenomena. Most ionic EAPs can be classified into conductive polymers (CPs) and IPMC, polymer gels, and carbon nanotubes.

An electronic type EAP-based strain sensor was fabricated by using silver-coated conductive fabric as an electrode and silicone rubber as a dielectric film. This sensor was able to capture elbow motion precisely but low capacitive (*pF* range) and strain value restrict its use in a wide range of applications.

To overcome this problem Ionic type of EAP-based sensor was fabricated, and efforts were directed to prepare free-standing stretchable polymer films to make capacitance strain sensors while introducing conducting polymers to make hybrid films with controlled conductivity and carbon grease was used as an electrode.

Conducting dielectric film increased the capacitance drastically (in μF range) and the sensor was showing a higher value of fracture strain. Further by using the crack growth approach, it was estimated that this sensor can sustain millions of cycles. Different electrical and mechanical characterizations (including sensor modeling like hyperelastic, and viscoelastic) have been performed and it was found that this sensor is suitable for wearable applications.

4.2 Experimental

4.2.1 Materials and methods

In this work, Ionic sensor was fabricated by utilizing conducting and elastic films having Styrene-Ethylene-Butylene-Styrene (SEBS) rubber and dodecyl benzenesulfonic acid (DBSA) doped polyaniline composite.

Doping of DBSA was done for below combinations

- ✓ Undoped Rubber
- ✓ 2.5 % Polyaniline
- ✓ 5.0 % Polyaniline
- ✓ 10 % Polyaniline
- ✓ 20 % Polyaniline

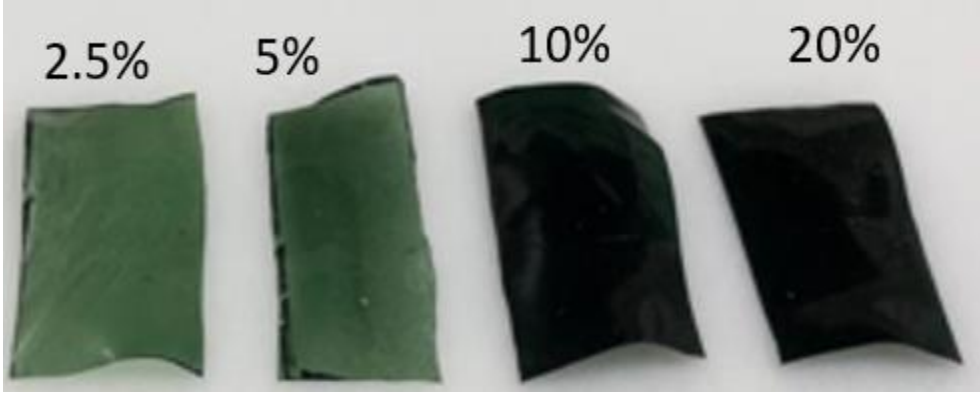

Fig. 1: DBSA doped dielectric film

In Fig. 1 DBSA doped films were fabricated at different concentrations.

4.2.2 Strain sensor fabrication

Sensor was fabricating by sandwiching DBSA doped polyaniline and Polystyrene-block-poly(ethylene-ran-butylene)-block-polystyrene-graft-maleic anhydride (SEBS-g-MA) composite film between two carbon grease electrodes.

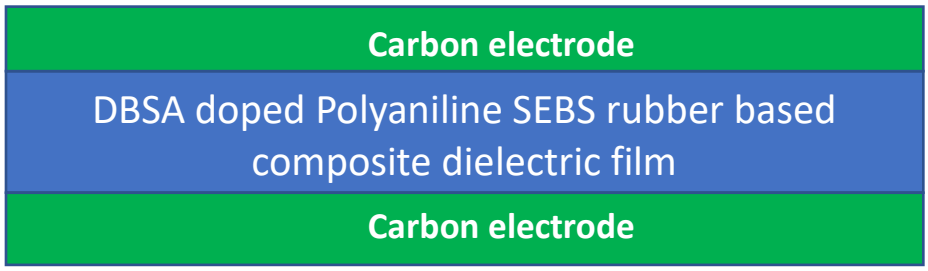

Fig. 2: Schematic diagram of strain senor

The capacitance of the DES under a relaxed state ($C_{relaxed}$) can be written as:

$$C_{relaxed} = \frac{\varepsilon_r \varepsilon_0 L_1 L_2}{L_3} \qquad (1)$$

Where, $L_1,\ L_2, L_3$ are the length, width and thickness of the sensor in an un-deformed state.

4.2.3 Tensile testing

4.2.3.1 Stress strain analysis

Stress strain was performed for mechanical characterization of sensor by using rectangular type of specimen

4.2.3.2 For estimating fatigue life

For fatigue life estimation edge crack specimen was used as shown in Fig.3. Here thickness of film was 0.22 mm. crack length was 5 mm. strain rate was 1mm/s. Here composite film was

fabricated by toluene solutions having 20% concentration. Here active length of sample was 17 mm and total width was 14 mm.

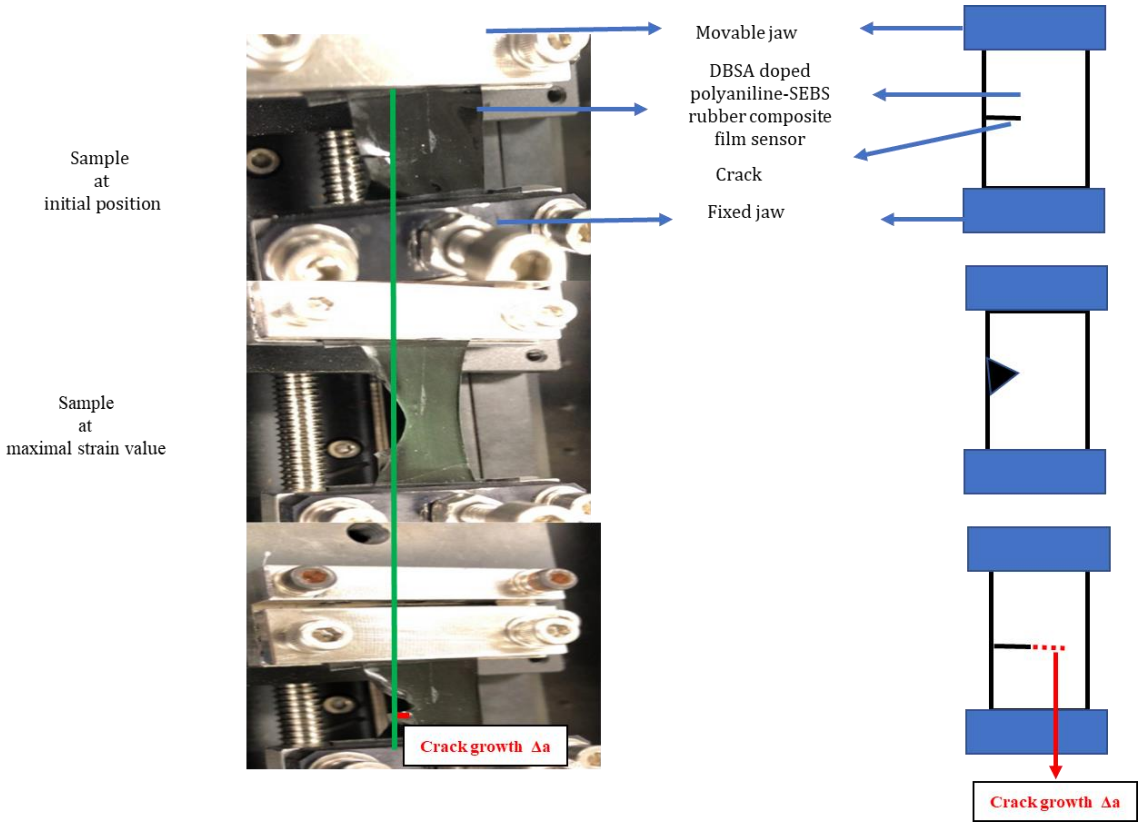

Fig. 3: Crack propagation in one complete cycle (left), Schematic diagram of the specimen subjected to cyclic loading unloading cycle with depiction of the crack growth Δa (right)

4.2.3.3 For estimation of tear strength

For estimating tear strength trouser type of specimen was use. Here speed of tensile machine was 1mm/s and thickness of film was 0.25 mm. Here composite film was fabricated by toluene solutions having 20% concentration

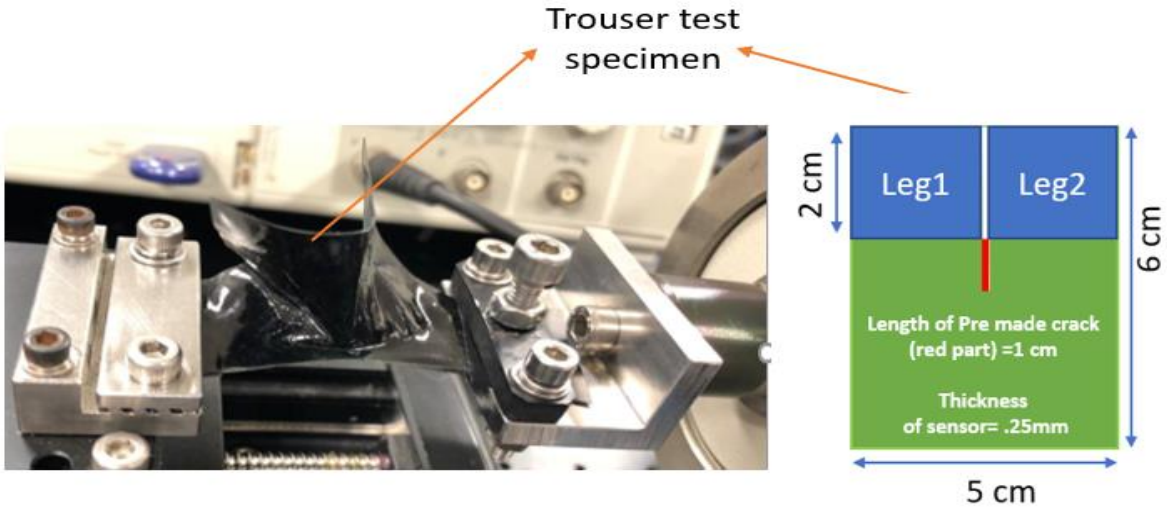

Fig. 4: (a) Trouser type of specimen fixed between two jaw of uniaxial tensile machine (left) Trouser specimen geometry (right)

4.3 Results and discussion

4.3.1 Electrical characteristics

It was found that, at relaxed state for undoped film, capacitance range was between 31 to 87 pF, as shown in Fig. 5 (left) while for doped film at 20% concentration and at 100% stretched state, capacitive range was between 40 to 99 µF due to increasing dielectric constant of doped film. These results indicate that, at relaxed and at stretched state, almost 10^6 times enhancement in capacitive response was attainable. Here rectangular type of sensor having 3 cm active length, 1.5 cm width and 0.05 mm thickness was used for measuring capacitance.

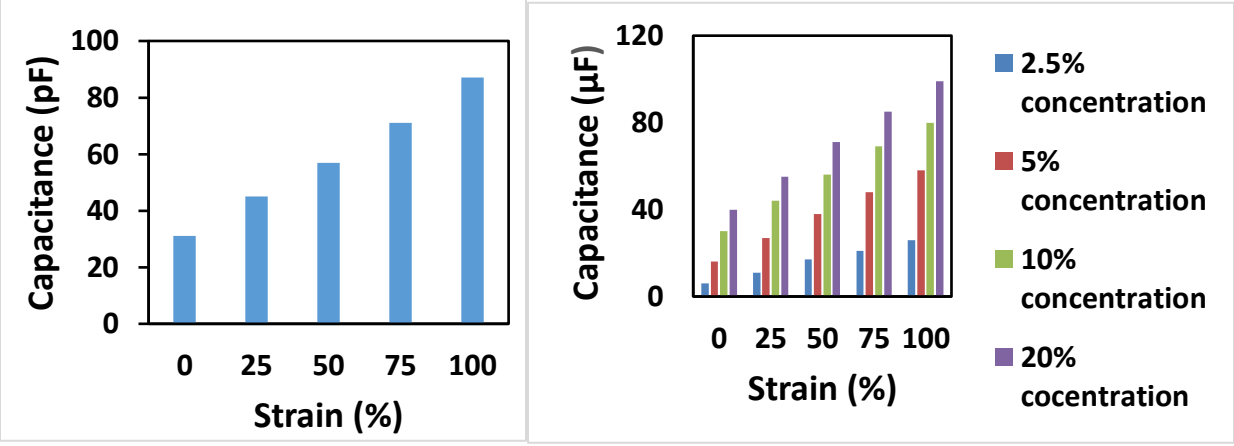

Fig. 5: Capacitance change at different strain value for undoped (left) and doped film (right)

In ionic type of EAP base capacitance is also quite high as compare to electronic EAP based strain sensors.

4.3.2 Mechanical characteristics

4.3.2.1 Elongation at break.

All doped films were highly stretchable (350 to 400% of initial length). Here speed of tensile machine was 1mm/sec Results are encouraging and composite film is suitable for soft robotic applications. Here rectangular type of sensor having 2 cm active length, 1 cm width and 0.2 mm thickness was used for elongation at break test.

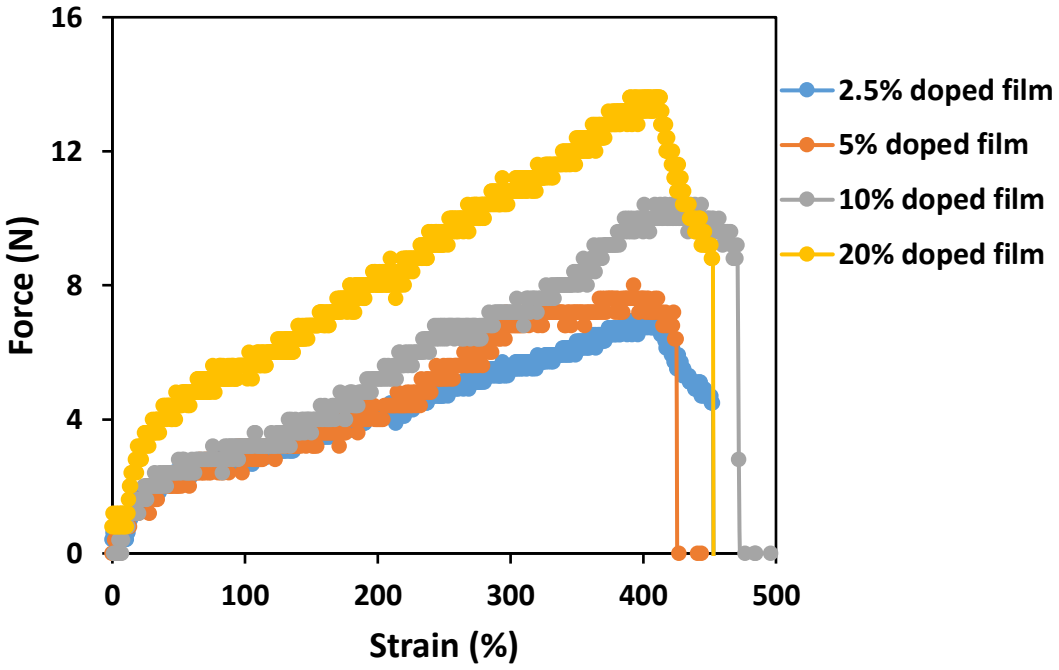

Fig. 6: Elongation at break characteristics

4.3.2.2 Hyperplastic characteristics

Fig.7 shows relationship between stress and strain of a unnotched sample at 100% strain over 5 loading-unloading cycles at strain rate 1 mm/sec. It can be seen from this figure that native film without crack exhibit reproducible and repetitive stress-stain curve confirming that Mullins's effect can be neglected and material can be considered purely elastic. Here rectangular type of sensor having 17 mm active length, 14 mm width and 0.22 mm thickness was used for mechanical characterization.

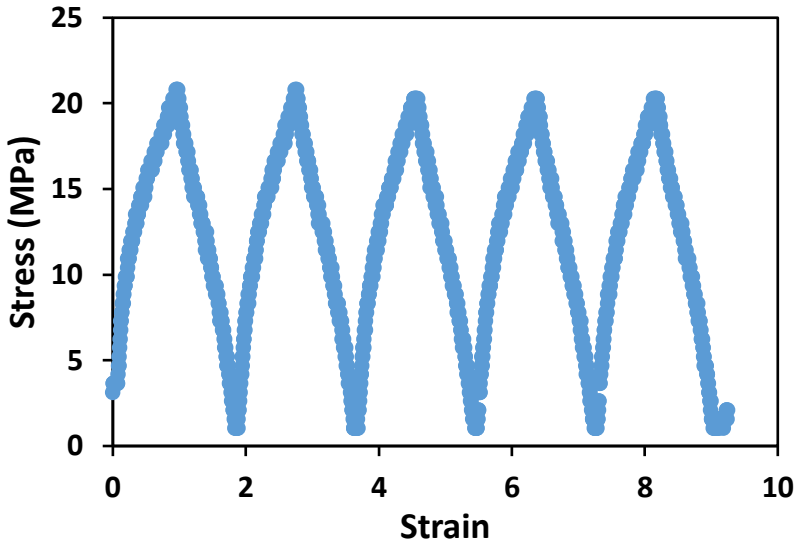

Fig. 7: Stress -strain curve at 100% value of strain

Stress can be calculated from equations given below,

$$\text{Stress}(\sigma)=\frac{F}{W*t} \qquad (2)$$

$$\text{Strain}\ (\epsilon)=\frac{\Delta L}{L} \qquad (3)$$

Where, σ is stress, ϵ is strain, F is force, w is width of specimen, t is thickness, ΔL is change in length, L is initial length.

4.3.2.3 Fatigue life prediction of film

Electroactive polymers (EAPs) with highly degree of elasticity in combination with electromechanical effect has made them very attractive for sensor application in the diverse areas such as soft robotics, human motion detection, virtual/augmented reality systems, entertainment industry, health monitoring, wearable devices [1-7]. Based on the principle of a variable parallel plate capacitor, EAP strain sensor can be fabricated utilizing an EAP layer sandwiched between two compliant electrodes. The capacitance changes during stretching and relaxation could be utilized for the monitoring and evaluation of the sensor performance.

In most of the areas, Electroactive polymer sensor undergoes loading and unloading cyclic operation, leading to a small initial defect like fatigue crack, flaws, notches, impurities, etc., which may grow to a critical size to induce catastrophic failure. For utilizing the Electroactive polymer strain sensors for long life span, it is quite necessary to estimate the mechanical life of EAP strain sensor.

In the conventional approach, fatigue life can be estimated from Wöhler curves (S-N curve, stress -number of strain cycles) but this method is very complex in terms of need for the large number of samples and time-consuming process [8-10]. Therefore, later crack growth-based approaches were proposed to predict the fatigue life quickly and simply (crack growth approach is used for estimating the length of a fatigue crack growing under cyclic loading and unloading cycles)**.** In the late 50's researchers adapted this method for rubbers, lately after minor improvements this approach has been adapted to multi-axial loading as well [11]. In 2017, Fan et al. predicted fatigue life of dielectric elastomers by using the crack growth approach [12]. Crack growth approach is a fast methodology to predict fatigue life of Rubber and day by day, it is getting popular in rubber industry. Incorporation of the doped conducting polymer in the stretchable insulating polymer matrix not only impart electrical conductivity but also enhances dielectric constant as well as mechanical robustness, which is suitable for the capacitive strain sensing applications [13-15]. Using this crack growth propagation, there are no report for the prediction of the fatigue life of for doped conducting polymer film-based sensors so far.

In this chapter we are first to successfully tested this crack growth approach for the strain sensor based on the stretchable freestanding composite film of SEBS rubber and DBSA doped polyaniline in order to predict the fatigue life of sensor. In this chapter, edge crack specimens have been used

to analyze the kinetics of crack growth under uniaxial loading and unloading cycles and followed the approach proposed by A.G. Thomas et al [16]. The power-law relation between the crack propagation rate (*da/dN)* and the tear energy (*T)* has been established for predicting the fatigue lifetime of the sensor.

For consideration of the better and reliable data, we chose 5th loading cycle of Fig. 7 (because crack propagate in loading cycle) for post treatment (as shown in Fig. 8).

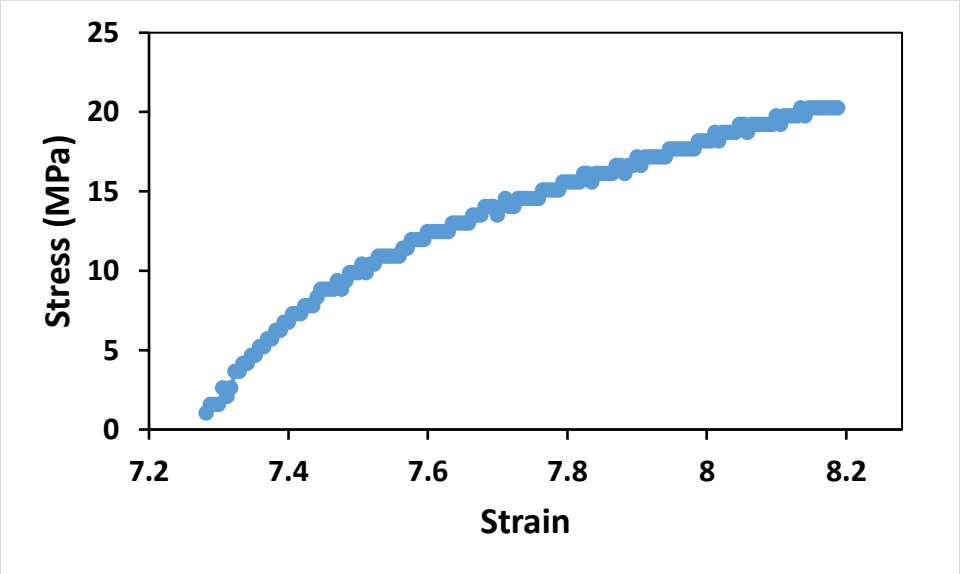

Fig. 8: Stress -strain curve at 100% value of strain

Mechanical energy per unit volume consumed by the material in straining to that limit is called strain energy density can be calculated by the eq. (4).,

$$\frac{W}{V} = \int \frac{F}{A_0}\frac{dL}{L_0} = \int_0^{\varepsilon} \sigma d\varepsilon \qquad (4)$$

Here V is volume, F is force L_0 is initial length, σ is stress ε is strain. From above equation we can conclude that W can be extracted by calculating the area under the stress-strain curve of a specimen without a precut. From eq. (4), we can see that area under stress -strain curve will directly give the strain energy density (W).

As we know that in a single edge cut, simple tension specimen, the energy release rate *T* (minimum energy required for tearing of sample), a strain dependent parameter k, the size of the crack a, strain energy density W, can be linked together by the formula as given below,

$$T = 2kWa \tag{5}$$

The dependence of the parameter *k* on strain was observed by Greensmith and Lindley can be calculated from formula given as below,

$$k = \frac{2.95 - .08\varepsilon}{\sqrt{(1+\varepsilon)}} \tag{6}$$

We calculated area under this stress – strain curve and after putting the all values in eq. (5) we calculated the tear energy of 1000 Joule/m^2, which is in a good agreement with value reported in literature also [17-19].

Fatigue life is determined by a pre-existing flaw in virgin unnotched sample. When it undergoes under loading and unloading cycles, firstly, this flaw grows to a critical size then material fails. The life of specimen can be calculated by integrating the growth rate of the growing flaw, from its initial length to critical length and relationship between crack propagate rate da⁄dN and the tearing energy *T* can be expressed by power-law behavior as given below,

$$\frac{da}{dN} = BT^F \tag{7}$$

Where, B and F are the material parameters can be calculated from curve fitting between experimental values and power-law modelling. Literatures show F may vary between 2 and 6 while B can change drastically.

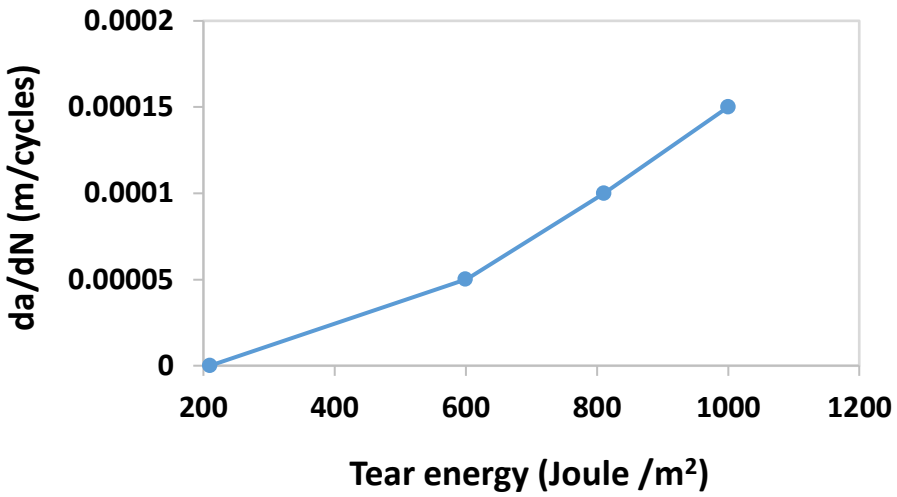

Fig. 9: Crack growth rate da/dN as a function of tear energy

As discussed earlier, the crack growth rate *da/dN* has been calculated by average of the crack growth Δa over 10 cycles.

As we know that the tearing energy T varies as a function of the strain value as explained above, therefore, we calculated tearing energy at different strain values. Consequently, the power-law mentioning the relationship between the tearing energy T and the crack growth rate can be explained from Fig.9.

The relationship between the tearing energy T and the crack growth as shown in Fig.9, can be fitted according to power law. We fitted the relationship between da/dN and T with power law and calculated the value of B $=5.65*10^{-11}$ and F= 2.1, which has been summarized in the Table 1 in order the compare our results with the reported values for other systems in the literature.

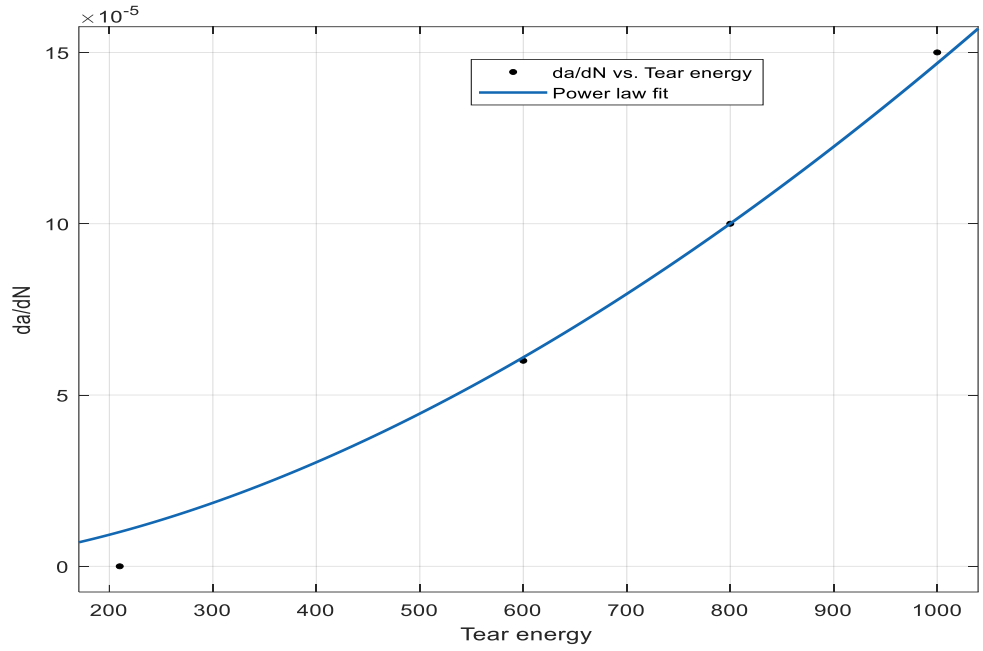

Fig. 10: Crack growth rate da/dN as a function of tear energy fitted to power law

Table 1: Material constants B and F for different rubbers [20-22]

Material name	Material constants		Authors
	B(m/cycles)/(J/m^2)	F	
Natural rubber (NR)	4.46×10^{-12}	1.35	Mars et al[20]
NR Filled with 23% carbon black	1.36×10^{-11}	1.93	Papadopoulos et al[21]
NR filled with 31% of carbon black and 9.5% plasticizer	4×10-14	2	Zarrrin et al[22]
DBSA doped polyaniline-SEBS rubber composite film	5.65×10^{-11}	2.1	Our work

Above graph is well fitted with the power law with a good fitting confidence of R^2= 99%, showing good agreement with literature also.

After putting the value of *T* in eq. (7), it becomes,

$$\frac{da}{dN} = B(2KWa)^F \quad (8)$$

After integration fatigue life , N_f can be calculated by the equations as shown below,

$$N_f = \int_0^{N_f} dN = \int_{a_0}^{a_f} \frac{da}{BT^F} \quad (9)$$

In above equation a_0 is initial flaw size and a_f is final or critical flaw size

$$N_f = \int_{a_0}^{a_f} \frac{da}{B(2KWa)^F} \quad (10)$$

$$N_f = \frac{1}{(F-1)B(2KW)^F {a_0}^{F-1}} \left[\frac{1}{{a_0}^{F-1}} - \frac{1}{{a_f}^{F-1}}\right] \quad (11)$$

If the initial crack length a_o is much smaller than the final crack length, a_f, then the fatigue lifetime becomes independent of the final crack length. Here a_0 can vary from 20 µm up to 50 µm. [20-24]

$$N_f = \frac{1}{(F-1)B(2KW)^F {a_0}^{F-1}} \quad (12)$$

After putting all values in equation 12, we found the fatigue lifetime of sensor is greater than 10^7 cycles, which shows sensor has a good fatigue life. We have observed that fatigue life time mainly depend upon B and F parameters and very less depend upon tear energy.

If the initial flaw size is considered as an intrinsic property of pristine material, and if variation of k with strain is neglected, then the constants of the eq. (12) may be combined into a single material constant C, as given by the eq. (13), which can be used to predict the fatigue lifetime of material easily.

$$N_f = CW^{-F} \quad (13)$$

4.3.2.4 Tear strength estimation of film

In recent years, a shift in the research trends from hard and brittle to soft, flexible, and light weight wearable devices has been noticed. Electroactive polymers (EAPs) strain sensors are the potential candidates for their application in the area of soft electromechanical wearable devices. During all electromechanical operations these sensors undergo repetitive large deformation so it becomes very important to estimate durability of EAP strain sensors. For evaluating durability of elastic materials mainly tear test is conducted on different type of specimen like: trouser, trapezoid and tongue type specimen. In this chapter we focused on trouser specimen-based tear test.

Basically, tear strength is a measure of resistance offered by elastomers itself against crack propagation. The tear strength has a significant impact on the prediction of life of elastomeric materials. In 1953 Rivlin and Thomas proposed the trouser test as a well-known method for determining the tear strength of elastomeric materials [25-28]. In 1974, Sawyers and Rivlin explained that in trouser test there are two legs are made by cutting a rectangular sample in the middle along its length and the force at which the pre-crack begins to grow is measured by pulling the legs in different directions [29-35]. But up to now there is a lack of papers on estimation tear strength of Electroactive polymer strain sensors, while Electroactive polymers strain sensors are widely used in soft robotics, rehabilitation, AR/VR technology and healthcare [36-40].

Electroactive polymers strain sensors are subjected to multiple and reversible stretching and relaxing cycles under different extents of the applied strains, therefore, it is very important to calculate the tear strength of these types of sensors as tear strength refers to the value of force required to rip a material until complete failure. The high value of tear strength shows material has the ability to withstand crack growth consequently crack propagation rate will be slow and the life of the material will be high.

In this chapter, a conducting and stretchable freestanding film consisting of SEBS rubber and dodecyl benzenesulfonic acid (DBSA) doped polyaniline composite film (belongs to ionic type of electroactive polymers family) was used for preparing a trouser type of specimen. Further tear test was conducted on this trouser type of specimen and tear strength was calculated. Later we have also calculated strain energy density for predicting the life of the specimen.

SEBS rubber was supplied from the Sigma-Aldrich co. while carbon grease was purchased from MG chemicals. DBSA doped polyanine was synthesized by reported procedure [40-48]. A stable suspension of the SEBS rubber and DBSA-doped polyanine was prepared by toluene. This suspension was used to prepare freestanding composite film with the thickness of 250 μm by solution casting. Further carbon grease coating was conducted on both sides of film.

Trouser type of specimen was used for determining the tear strength of sensor of sensor having 1 cm pre-cut. Both legs of sensor were fixed between two jaw of tensile testing machine as shown in the Fig. 1. Tensile testing system consists of a 100 N load cell, one end movable and another fixed, X-Y stage controller and an Oscilloscope.

Using a stage controller and a movable jaw tearing data was recorded by computer using a LabView program. After running the tearing test 1mm/s), the legs of trouser specimen were pulled apart in opposite direction for initializing tearing action of sensor. In Fig 1(b) blue parts denote the leg of specimen (20 mm), red part is pre-crack length (10 mm). Total length of sensor was 60 mm while 20mm was used for clamping purpose. Total length, thickness and width of sensor was 60 mm and 0.25 mm and 50 mm, respectively.

Tear test has been widely used to evaluate the tear propagation resistance of a various types of polymeric and elastomeric films. In this work, our in house custom-made tensile measurement system was used for the tear test of the conducting composite film, where the force required to propagate an initially created crack in the trouser type specimen was measured. Figure 2 shows relationship between tear strength and displacement of pre-crack trouser type specimen at 1 mm/s speed. Further with the help of equation 4, tear strength (T) was evaluated.

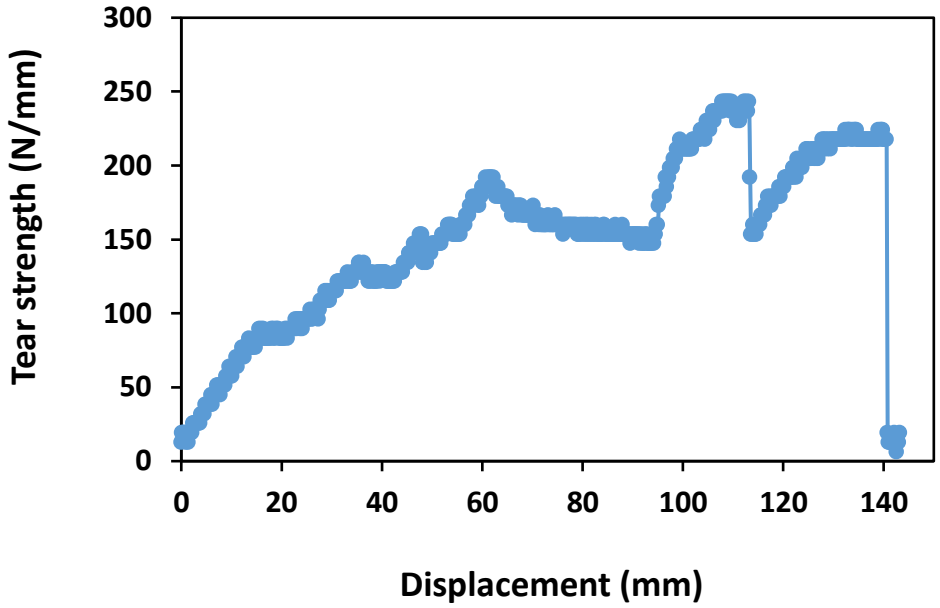

Fig. 11: Tear strength vs displacement for trouser type specimen

It can be seen from the Fig. 11 that tear path is not straight and follows a zigzag path, which was concluded by the observation that total displacement to be more than the original length of sample. For calculating tear strength of film, we calculated average value of tear strength as shown in the Fig. 11, which was approximately 150N/mm. This indicates that the sensor exhibits fairly good tear strength and can sustain a large loading and unloading cycles. Life of a specimen under reversible loading and unloading cycles at a fixed applied strain can also be predicted using following equation:

$$N_f = \frac{1}{(F-1)B(2KW)^F {a_0}^{F-1}} \qquad (14)$$

Where, N_f is predicted life of specimen. B and F are material parameters and can be calculated from power law, for same material value of B and F can be considered constant. a_0 is initial flaw size and varies from 20 μm up to 50 μm [21-22]. k is strain dependent constant can be calculated by below mentioned formula

$$k = \frac{2.95-.08\varepsilon}{\sqrt{(1+\varepsilon)}} \qquad (15)$$

W is mechanical energy per unit volume at the stretched state, which is also called strain energy density. W can be calculated by the eq. (16).

$$W = \int \frac{F}{A_0}\frac{dL}{L_0} = \int_0^{\varepsilon} \sigma d\varepsilon \qquad (16)$$

Where, L_0 *and* A_0 are initial length and cross-section area, stress, strain respectively. From the eq. (16), we can conclude that W can be evaluated by calculating area under the curve of stress strain obtained from the trouser tear test. Stress-strain curve for tearing the pre-cracked trouser type of sensor specimen used for present investigation has been shown in the Fig. 12

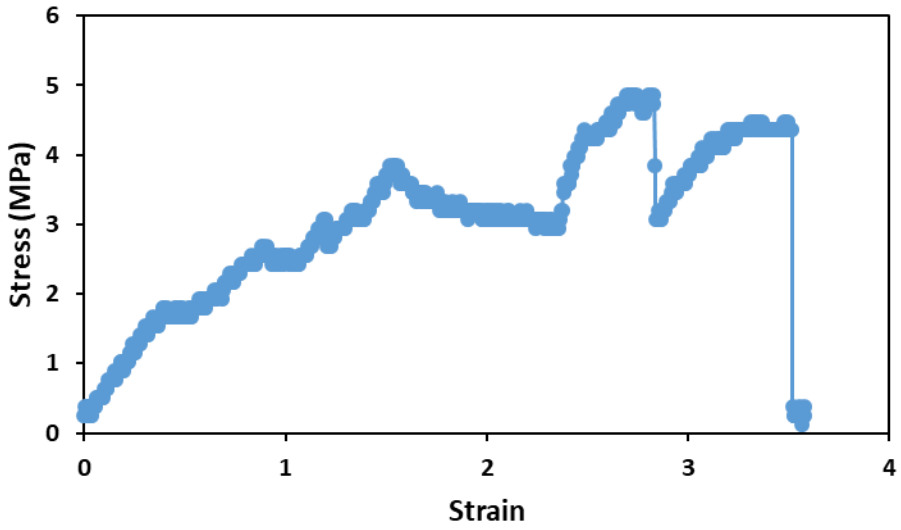

Fig. 12: Stress strain curve obtained from trouser tear test

Area under stress strain curve also known as strain energy density was estimated to be 10.8 N/mm^2. Nitin et al have calculated B=5.65×10^{-11}and F = 2.1 for the same sensor [25]. Utilizing the eq. (15), estimated value W along with material constants B and F, it was estimated that sensor can sustain life cycles in the range of 10^7 at an applied strain of 100%. This confirms that this sensor has good value of tear strength and offering huge resistance during tearing means this sensor is showing very slow crack growth during the tear test

4.4 Conclusion

Sensor is showing very good mechanical and electrical properties. Sensor showing large enhancement in capacitance which is quite higher than electronic type of EAP sensors on the other hand sensor can sustain millions of cycles and can be elongate more than 400% shows this sensor has great potential in wearables.

4.5 References

[1] Huang, Bo, et al. "Wearable stretch sensors for motion measurement of the wrist joint based on dielectric elastomers." Sensors 17.12 (2017): 2708.

[2] Bar-Cohen, Yoseph, and Qiming Zhang. "Electroactive polymer actuators and sensors." MRS bulletin 33.3 (2008): 173-181.

[3] Kim, Kwang J., and Satoshi Tadokoro. "Electroactive polymers for robotic applications." Artificial Muscles and Sensors 23 (2007): 291.

[4] Singh, Nitin Kumar, Kazuto Takashima, and Tomohiro Shibata. "Dielectric elastomer based stretchable textile sensor for capturing motion." Electroactive Polymer Actuators and Devices (EAPAD) XXII. Vol. 11375. International Society for Optics and Photonics, 2020.

[5] Rosenthal, Marcus, et al. "Applications of dielectric elastomer EPAM sensors." Electroactive Polymer Actuators and Devices (EAPAD) 2007. Vol. 6524. International Society for Optics and Photonics, 2007. Biddiss, Elaine, and Tom Chau. "Electroactive polymeric sensors in hand prostheses: Bending response of an ionic polymer metal composite." Medical engineering & physics 28.6 (2006): 568-578.

[6] Chen, Jianwen, et al. "An overview of stretchable strain sensors from conductive polymer nanocomposites." Journal of Materials Chemistry C 7.38 (2019): 11710-11730.

[7] Singh N. K., Patra K., Kumar A. “Energy harvesting using Dielectric Elastomer”, International conference on advanced materials for power engineering (ICAMPE-2015), 11-13 December 2015, Kerala, India

[8] Wöhler, Alfred. About strength tests with iron and steel. Ernst & Korn, 1870.

[9] Murakami, Yukitaka, et al. "Essential structure of SN curve: Prediction of fatigue life and fatigue limit of defective materials and nature of scatter." International Journal of Fatigue 146 (2021): 106138.

[10] Andriyana, Andri, and Erwan Verron. "Prediction of fatigue life improvement in natural rubber using configurational stress." International Journal of Solids and Structures 44.7-8 (2007): 2079-2092.

[11] Harbour, Ryan J., Ali Fatemi, and Will V. Mars. "Fatigue life analysis and predictions for NR and SBR under variable amplitude and multiaxial loading conditions." International Journal of Fatigue 30.7 (2008): 1231-1247.

[12] Fan, Wei, Yang Wang, and Shengqiang Cai. "Fatigue fracture of a highly stretchable acrylic elastomer." Polymer Testing 61 (2017): 373-377.

[13] Kang, Sehong, et al. "A Flexible Patch-Type Strain Sensor Based on Polyaniline for Continuous Monitoring of Pulse Waves." IEEE Access 8 (2020): 152105-152115.

[14] Chen, Jing, et al. "Super stretchable electroactive elastomer formation driven by aniline trimer self-assembly." Chemistry of Materials 27.16 (2015): 5668-5677.

[15] Huang, Yao, et al. "Conductive polymer composites from renewable resources: an overview of preparation, properties, and applications." Polymers 11.2 (2019): 187.

[16] Rivlin, R. S., and A. G. Thomas. "Rupture characteristic of rubber for tearing energy." Polymer Science 10.3 (1953): 291.

[17] Kollosche, Matthias, et al. "Strongly enhanced sensitivity in elastic capacitive strain sensors." Journal of Materials Chemistry 21.23 (2011): 8292-8294.

[18] Adams, P. N., P. J. Laughlin, and A. P. Monkman. "Synthesis of high molecular weight polyaniline at low temperatures." Synthetic Metals 76.1-3 (1996): 157-160.

[19] M. Pharr, Y.J. Sun, Z. Suo, Rupture of highly stretchable acrylic dielectric elastomer, J. Appl. Phys. 111 (2012)

[20] W.V. Mars, Factors that affect the fatigue life of rubber: a literature survey, J. Rubb. Chem. and Tech., 77,391-412 (2004)

[21] Papadopoulos, Ioannis. Predicting the fatigue life of elastomer components. Diss. Queen Mary, University of London, 2006.

[22] Zarrin Ghalami. Fatigue life prediction and modeling of elastomeric components (Doctoral dissertation, University of Toledo).

[23] Mars, W. V., and A. Fatemi. "A literature survey on fatigue analysis approaches for rubber." International Journal of fatigue 24.9 (2002): 949-961.

[24] Rivlin RS, Thomas AG. Rupture of rubber. I. Characteristic energy for tearing. Journal of polymer science. 1953 Mar;10(3):291-318.

[25] Sawyers KN, Rivlin RS. The trousers test for rupture. In collected papers of RS Rivlin 1997 (pp. 2643-2648). Springer, New York, NY.

[26] Pissarenko A, Yang W, Quan H, Poyer B, Williams A, Brown KA, Meyers MA. The toughness of porcine skin: Quantitative measurements and microstructural characterization. journal of the mechanical behavior of biomedical materials. 2020 Sep 1; 109:103848.

[27] Singh N.K., Takashima K., Shibata T., "Dielectric elastomer based stretchable textile sensor for capturing motion." Electroactive Polymer Actuators and Devices (EAPAD) XXII. Vol. 11375. International Society for Optics and Photonics, 2020.

[28] Singh N.K, Patra K., "Modeling and Experimental Study of Dielectric Elastomer based Energy Scavenging System", International Conference on Polymer and Allied Materials (ICPAM 2014), 30-31 May 2014, Patna, India.

[29] Singh N. K., Kazuto T., and Pandey S.S., *"*Human Body Posture Recognition using Electroactive Polymer Based Strain Sensor*"*.8th International Symposium on Applied

Engineering and Sciences (SAES2020) Kyushu Institute of Technology, 12th – 19th Dec 2020

[30] Singh N.K., Patra K., Kumar A., “Energy harvesting using Dielectric Elastomer”, International conference on advanced materials for power engineering (ICAMPE-2015), 11-13 December 2015, Kerala, India

[31] Singh N. K., Kazuto T., and Pandey S.S., “DBSA Ion doped Polyaniline-SEBS Rubber Composite Film as Stretchable Capacitive Sensor for Soft Robotic Applications”. 30th Annual Meeting of Japan Materials Research Society, Yokohama (online), December 9-11, 2020.

[32] Singh N.K., "Energy harvesting using dielectric elastomer”, Master thesis under the guidance of Patra K. –Indian institute of technology Patna- India (2014).

[33] Higueras-Ruiz DR, Nishikawa K, Feigenbaum H, Shafer M. What is an artificial muscle? A comparison of soft actuators to biological muscles. Bioinspiration & biomimetics. 2021 Dec 23;17(1):011001.

[34] Zhu Y, Giffney T, Aw K. A Dielectric Elastomer-Based Multimodal Capacitive Sensor. Sensors. 2022 Jan;22(2):622.

[35] Xiao, H., Wu, J., Ye, W., & Wang, Y. “Dynamic modeling for dielectric elastomer actuators based on LSTM deep neural network”. In 2020 5th international conference on advanced robotics and mechatronics (ICARM) 2020.

[36] Ye Z, Chen Z. “Self-sensing of dielectric elastomer actuator enhanced by artificial neural network”. Smart Materials and Structures, 26(9):095056,2017

[37] Kim D, Kim SH, Kim T, Kang BB, Lee M, Park W, Ku S, Kim D, Kwon J, Lee H, Bae J. “Review of machine learning methods in soft robotics”. 16(2): e0246102

[38] Larson C, Spjut J, Knepper R, Shepherd R., “A deformable interface for human touch recognition using stretchable carbon nanotube dielectric elastomer sensors and deep neural networks”. Soft robotics. 6(5):611-20,2019.

[39] Chiba S, Waki M, Fujita K, Song Z, Ohyama K, Zhu S. “Recent progress on soft transducers for sensor networks”. Technologies and Eco-innovation towards Sustainability II.285-98, 2019.

[40] Zeng X, Deng HT, Wen DL, Li YY, Xu L, Zhang XS. Wearable Multi-Functional Sensing Technology for Healthcare Smart Detection. Micromachines.13(2):254,2022.

[41] Hannigan BC, Cuthbert TJ, Geng W, Tavassolian M, Menon C. Understanding the Impact of Machine Learning Models on the Performance of Different Flexible Strain Sensor Modalities. Frontiers in Materials 8,44. 2021.

[42] Kollosche, Matthias, et al. "Strongly enhanced sensitivity in elastic capacitive strain sensors." Journal of Materials Chemistry 21.23 (2011): 8292-8294.

[43] Adams, P. N., P. J. Laughlin, and A. P. Monkman. "Synthesis of high molecular weight polyaniline at low temperatures." Synthetic Metals 76.1-3 (1996): 157-160.

[44] W.V. Mars, Factors that affect the fatigue life of rubber: a literature survey, J. Rubb. Chem. and Tech., 77,391-412 (2004)

[45] Mars, W. V., and A. Fatemi. "A literature survey on fatigue analysis approaches for rubber." International Journal of fatigue 24.9 (2002): 949-961.

[46] Fan, Wei, Yang Wang, and Shengqiang Cai. "Fatigue fracture of a highly stretchable acrylic elastomer." Polymer Testing 61 (2017): 373-377.

[47] M. Pharr, Y.J. Sun, Z. Suo, Rupture of highly stretchable acrylic dielectric elastomer, J. Appl. Phys. 111 (2012)

[48] Singh N. K., Kazuto T., and Pandey S.S., "Fatigue life prediction of electroactive polymer strain sensor." Electroactive Polymer Actuators and Devices (EAPAD) XXIII. Vol. 11587. International Society for Optics and Photonics, 2021.

CHAPTER-5

APPLICATION IN WEARABLES

5.1 Introduction

A sensor is a device that is used to detect changes in environment and send the information to other electronic devices. Sensors can be classified based on the transduction mechanisms. The commercially available sensors include stretch sensors, pressure sensors, flow sensors, accelerometers, vibration sensors, temperature sensors, etc.

There are plenty of sensor technologies like piezo-resistive sensors, accelerometers/gyros, and camera systems, are available for capturing motion. All these technologies have plenty of drawbacks like: camera systems require structured environments with controlled lighting, piezo-resistive sensors lack precision and are environmentally sensitive, and accelerometers drift at low frequency etc. These technologies are complex, expensive and potentially obtrusive and bulky to wear and devices capable of measuring larger strains or displacements are usually much more complex. Therefore, in this paper we are presenting a dielectric elastomer based stretchable textile sensor, which overcomes the aforementioned problems and drawbacks.

In the recent past, dielectric elastomers (DE) based sensors have attracted considerable attention because of their potential in healthcare and soft robotics fields [1-4]. Dielectric elastomer-based stretch sensors have plenty of advantages over conventional sensors and compliant properties enable the DE based stretch sensors to safely monitor soft movements or interactions with humans [5-10]. DE based sensors can be used to measure strain, pressure, similar to the human skin, which have advantageous properties such as flexibility, highly sensitivity and technological compatibility with a large area [11-12].

Multimodal dielectric elastomer sensors can also sense humidity, temperature, as well as chemical and biological stimulation in human-activity monitoring and healthcare. There is a huge demand of capturing motion at large value of stain in human activity monitoring, virtual/augmented reality systems, entertainment sector, sports and fitness industries and DE based stretchable textile sensor can fulfil this demand [13-16]. In this paper DE based stretchable textile sensor's characteristics and complete technology for capturing motion have been explained. This type of sensor can easily

convert large mechanical strain into capacitance, consequently motion can be captured precisely even at large value of strain too [17-18].

5.2 Experimental

5.2.1 Materials and methods

5.2.1.1 Elbow motion for one cycle

In this work, fabric electrode-based sensor was used. Capacitance was measured by using electrometer. Sensor was fixed on elbow and protractor was used for measuring elbow's joint angle. Capacitance was measured for elbow bending (0 degree to 90 degree) and straightening (90 degree to 0 degree)

Fig. 1: Fabric electrode-based sensor fixed on elbow.

5.2.1.2 Elbow motion for multiple cycles

Elbow motion for multiple cycles was measured by using LEAP technology's sensor kit (Including sensors, software, electronics circuit etc).

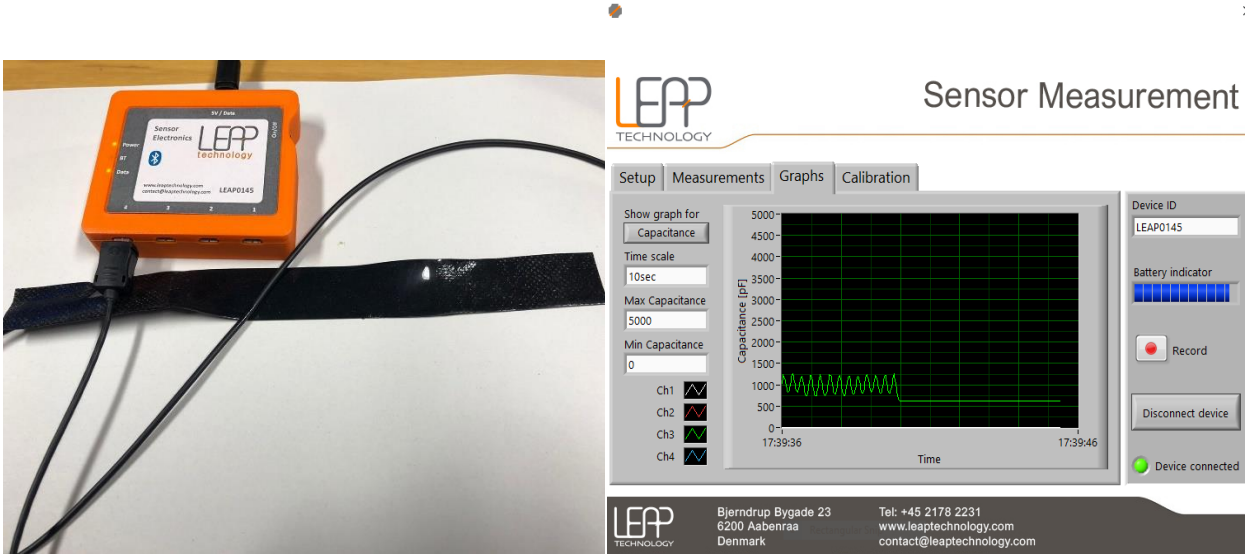

Fig. 2: LEAP technology's sensor kit

Fig. 3: LEAP technology's sensor fixed on elbow

5.2.1.3 Hand gesture recognition:

LEAP technology's sensors were attached on stretchable glove and connected to sensor kit for recording sensor data for 30 seconds in open hand and fist position of hand.

Fig. 4: LEAP technology's sensor fixed on stretchable glove for taking data for hand gesture recognition in open and fist position of hand

5.3 Result and discussion

5.3.1 Detecting elbow's position

Soft strain sensors can also be used for detecting human motion. Here we are explaining an example for detecting elbow motion. We can easily measure capacitance during sensor's stretched and relaxed state and with the help of basic calibration technique (between joint angles and capacitance) we can easily detect the elbow's position.

We fixed the electronic type of EAP based strain sensor on and bent the elbow at from 0 to 90 degree and straightened the elbow from 90 degree to 0 degree. Protractor was used to measure joint angle (elbow) and capacitance was used by using electrometer.

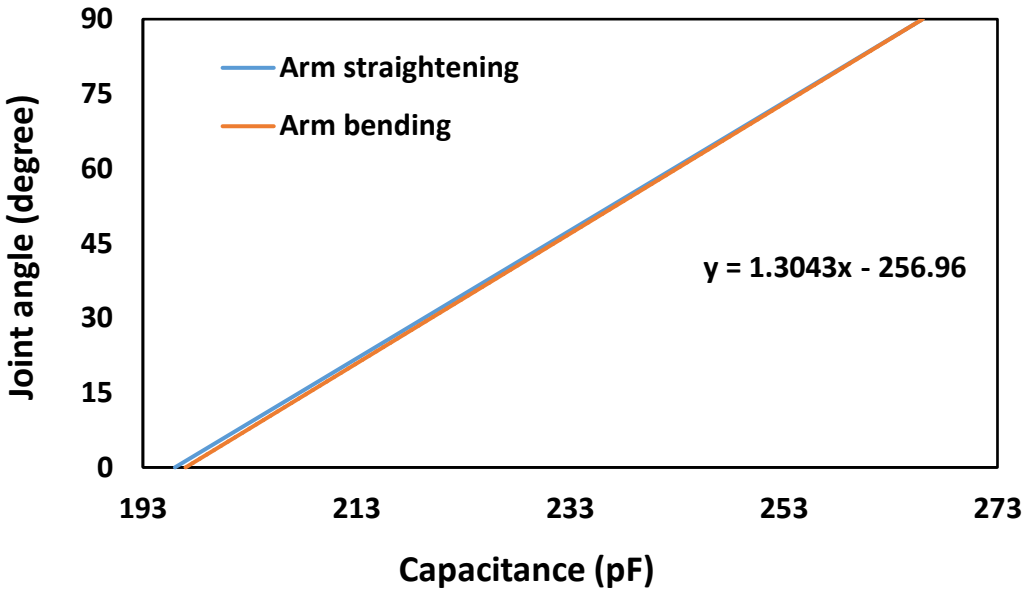

Fig. 5: Graph between joint angles and capacitance.

Capacitance during bending state and straightening state was recorded and graph was plotted between capacitance and joint (as shown in Fig. 5) angles. From above graph relation between joint angles and capacitance can be easily established. By using this relationship, elbow's position can be easily estimated using capacitive values only and vice versa is also true. In figure given below sensor data was collected for multiple cycles of elbow bending and straightening using LEAP technology's sensor kit.

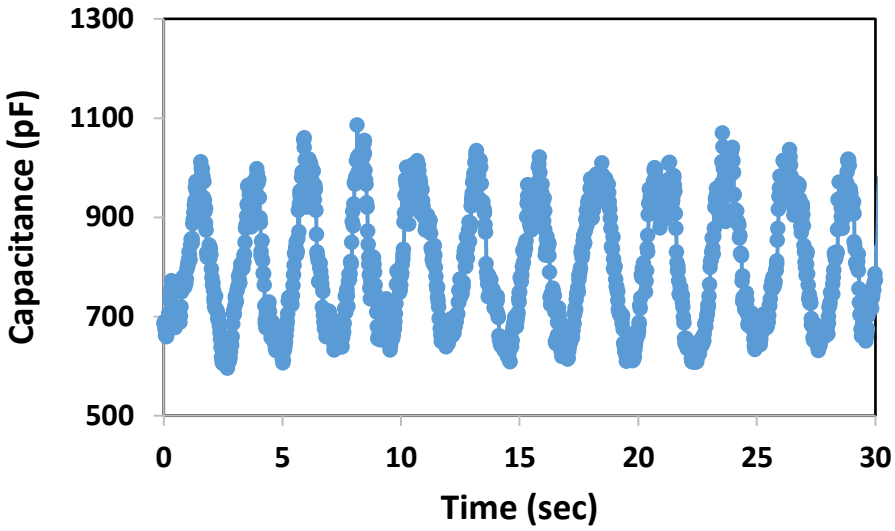

Fig. 6: Elbow motion for multiple cycles using LEAP technology's sensor kit

5.3.2 Hand gesture recognition

Sensors data was collected using LEAP sensor kit for open and fist position of hand. LEAP sensor kit has only four ports, can record only 4 sensor's data simultaneously so sensor data of 5th sensor was measured separately for open and fist position of hand for that particular finger and added this data in corresponding part of open and fist potion hand data of rest of 4 fingers.

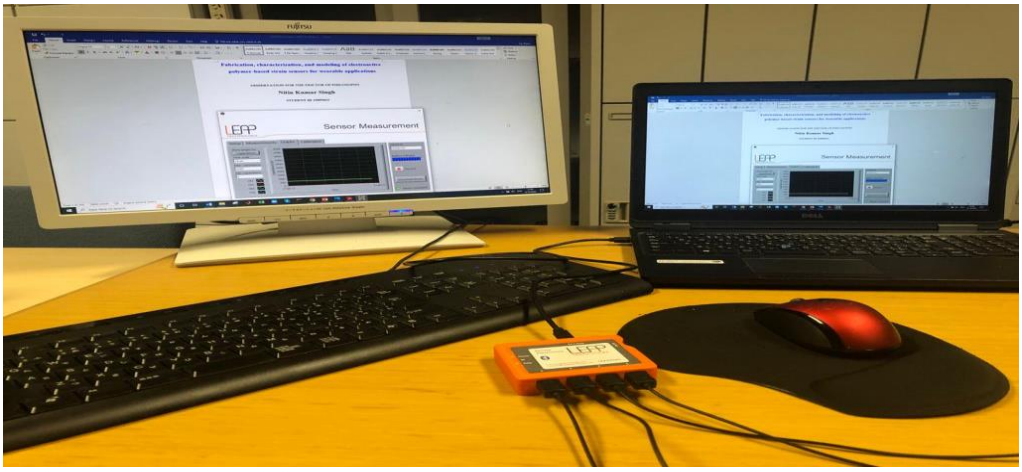

Fig. 7: Four sensors connected to LEAP technology's sensor kit

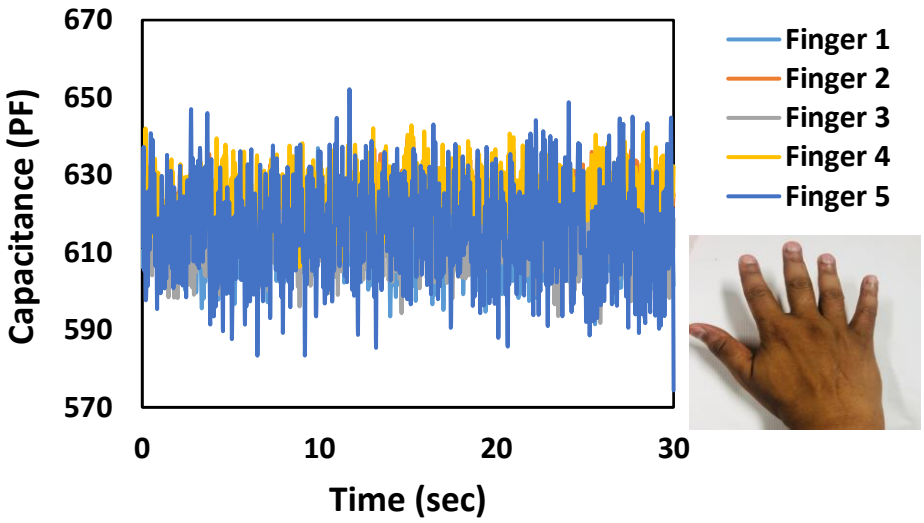

Fig. 8: Sensor data using LEAP technology's sensor kit for open hand position for 30 seconds

In Fig.8 we can see that range of capacitive bandwidth is varying from 600 pF to 630 pF (approximately), so if the size of hand is same (as used in collecting this data) then the bandwidth this capacitive range (600 pF to 630 pF) of hand gesture can be considered as open position.

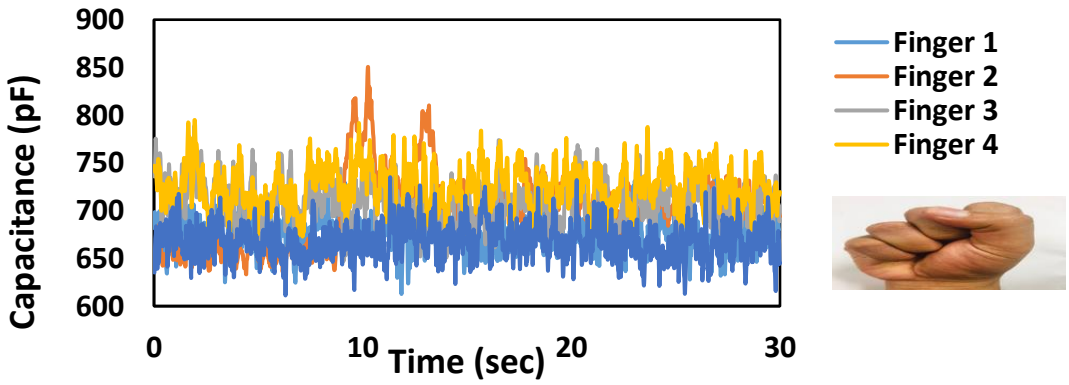

Fig. 9: Sensor data using LEAP technology's sensor kit for fist position of hand for 30 sec

In Fig.9 we can see that range of capacitive bandwidth is varying from 650 pF to 725 pF (approximately), so if the size of hand is same (as used in collecting this data) then the bandwidth of this capacitance range (between 650 pF to 725 pF) of hand gesture can be considered as a fist position.

5.4 Conclusions

Capacitance during elbow flexion and extension was measured using various types of EAP strain sensors (fabric and non-fabric electrode-based sensors). Relation between capacitance and joint angles was established by using mathematical linear equation as given in above figure, can be used for predicting elbow's position by measuring capacitance value. Sensor data was collected for open and fist type of hand gesture and a capacitive bandwidth was calculated which predict the type of gesture i.e. open hand or fist position (if size of user's hand is same as used in collecting data). EAP strain sensors have the potential to be widely used in human activity monitoring, rehabilitation, gesture recognition, Human commuter interface etc.

5.5 References

[1] Cohen, D.J., D. Mitra, K. Peterson, and M.M. Maharbiz, "A highly elastic, capacitive strain gauge based on percolating nanotube networks," Nano Letters, 12(4): p. 1821-1825. (2012)

[2] Assaf, T., J. Rossiter, and M. Pearson. "Contact sensing in a bio-inspired whisker driven by electroactive polymer artificial muscles," Sensors, 2013 IEEE (2013)

[3] Kim, D., C.H. Lee, B.C. Kim, D.H. Lee, H.S. Lee, C.T. Nguyen, U.K. Kim, T.D. Nguyen, H. Moon, J.C. Koo,J.D. Nam, and H.R. Choi. "Six-axis capacitive force/torque sensor based on dielectric elastomer," Proc. SPIE 8687, (2013)

[4] Kim, D.S., N. Huu Chuc, S.M. Jin, K.J. An, V.H. Phuc, J. Koo, Y. Lee, J.D. Nam, and H.R. Choi. "A flexible fingertip tactile sensor," Proc. SPIE 7642, (2010)

[5] Hu, W., X. Niu, R. Zhao, and Q. Pei, "Elastomeric transparent capacitive sensors based on an interpenetrating composite of silver nanowires and polyurethane," Applied Physics Letters, 102(8): p. 083303-083303-5. (2013)

[6] Rosenthal, M., N. Bonwit, C. Duncheon, and J. Heim. "Applications of dielectric elastomer EPAM sensors," Proc. SPIE 6524, (2007)

[7] Lipomi, D.J., M. Vosgueritchian, B.C.K. Tee, S.L. Hellstrom, J.A. Lee, C.H. Fox, and Z. Bao, "Skin-like pressure and strain sensors based on transparent elastic films of carbon nanotubes," Nature Nanotechnology, 6(12): p. 788-792. (2011)

[8] Iskandarani, Y. and H.R. Karimi, "Sensing Capabilities Based on Dielectric Electro Active Polymers; Feasibility and Potential State-of-the-Art Application," Sensors Journal, IEEE, 12(8): p. 2616-2624. (2012)

[9] York, A., J. Dunn, and S. Seelecke, "Systematic approach to development of pressure sensors using dielectric electro-active polymer membranes," Smart Materials and Structures, 22(9). (2013)

[10] Kollosche, M., H. Stoyanov, S. Laflamme, and G. Kofod, "Strongly enhanced sensitivity in elastic capacitive strain sensors," Journal of Materials Chemistry, 21(23): p. 8292-8294. (2011)

[11] Buchberger, G., B. Mayrhofer, B. Jakoby, W. Hilber, and S. Bauer. "Dynamic capacitive extensometry setup for in-situ monitoring of dielectric elastomer actuators," IEEE I2MTC 2012 75-80, (2012)

[12] Charalambides, A. and S. Bergbreiter. "All-elastomer in-plane MEMS capacitive tactile sensor for normal force detection," Sensors, IEEE (2013)

[13] Lacour, S.P. and D.P.J. Cotton. "Elastomeric capacitive sensors," transducers 2011 2770- 2773, (2011)

[14] Ponce Wong, R.D., J.D. Posner, and V.J. Santos, "Flexible microfluidic normal force sensor skin for tactile feedback," Sensors and Actuators, A: Physical, 179: p. 62-69. (2012)

[15] Roberts, P., D.D. Damian, S. Wanliang, L. Tong, and C. Majidi. "Soft-matter capacitive sensor for measuring shear and pressure deformation," IEEE ICRA 2013 3529-3534, (2013)

[16] Toth, L.A. and A.A. Goldenberg. "Control system design for a dielectric elastomer actuator: The sensory subsystem," Proc. SPIE 4695, (2002)

[17] Nitin Kumar Singh, Karali Patra, A. Kumar "Energy harvesting using Dielectric Elastomer", International conference on advanced materials for power engineering (ICAMPE-2015), 11-13 Dec 2015, Kerala, India

[18] Singh, Nitin Kumar, Kazuto Takashima, and Shyam Sudhir Pandey. "Electronic versus Ionic Electroactive Polymers (EAPs) Strain Sensors for Wearable Electronics: A Comparative Study." *Engineering Proceedings* 21.1 (2022): 1.

CHAPTER-6

GENERAL CONCLUSION

AND

FUTURE PROSPECTS

6.1 General conclusion

Wearable sensors add significant value to many wearable electronic devices like smartwatches and fitness tracking systems etc. Gradually trend is shifting towards soft and flexible devices based on wearable sensors for use in applications like health and fitness, medical, and AR/VR. In this present research, a systematic comparison has been made by fabricating the electronic and ionic types of capacitive EAP strain sensors. To accomplish this, a combination of silicone rubber sandwiched between silver-coated stretchable electrodes is used as an electronic type of EAP sensor, while a conducting and stretchable freestanding film consisting of SEBS rubber and DBSA doped polyaniline composite film sandwiched between carbon grease electrodes is chosen as an ionic type of EAP sensor. Mechanical characterization in terms of the uniaxial tensile testing was performed on both types of sensors using our custom-made tensile testing system, while capacitance under reversible stretching and relaxation under variable strains was measured by using a computer-controlled XY-stage and an electrometer. Constitutive equations based on various existing mathematical models were used for analyzing stress-strain curves obtained from uniaxial tensile testing for predicting the mechanical behavior of the sensor in multiaxial loading. It was found that observed capacitance was dramatically enhanced for the ionic sensors. Conducting fabric used as stretchable top and bottom electrodes limit the elasticity of the sensor, while the ionic type of sensor can be stretched more than twice of fabric-based sensors. Open and fist hand gesture was also recognized using commercial sensor kit.

6.2 Future prospects

Regarding sensor fabrication part, as discussed in previous chapter that fabric-based electrode limits the elasticity of sensor on the other hand carbon grease-based electrodes are not suitable for commercialization purpose due to its numerous drawbacks. In chapter 3 we have increased the base value of capacitance by using DBSA doped polyaniline composite film but we used carbon grease electrode for testing the performance of sensor, in future possibility of composite type of electrodes like combination of liquid silicone and carbon or silver can be explored for fabrication DBSA doped ionic sensors.

Regarding application part, the research work conducted for this thesis has demonstrated the importance of the hand gesture recognition which has sparked a lot of research as a crucial method for human-machine interaction. By attaching sensors on the hand or integrating them into hand gloves, strain sensors can play an important role in gesture recognition.

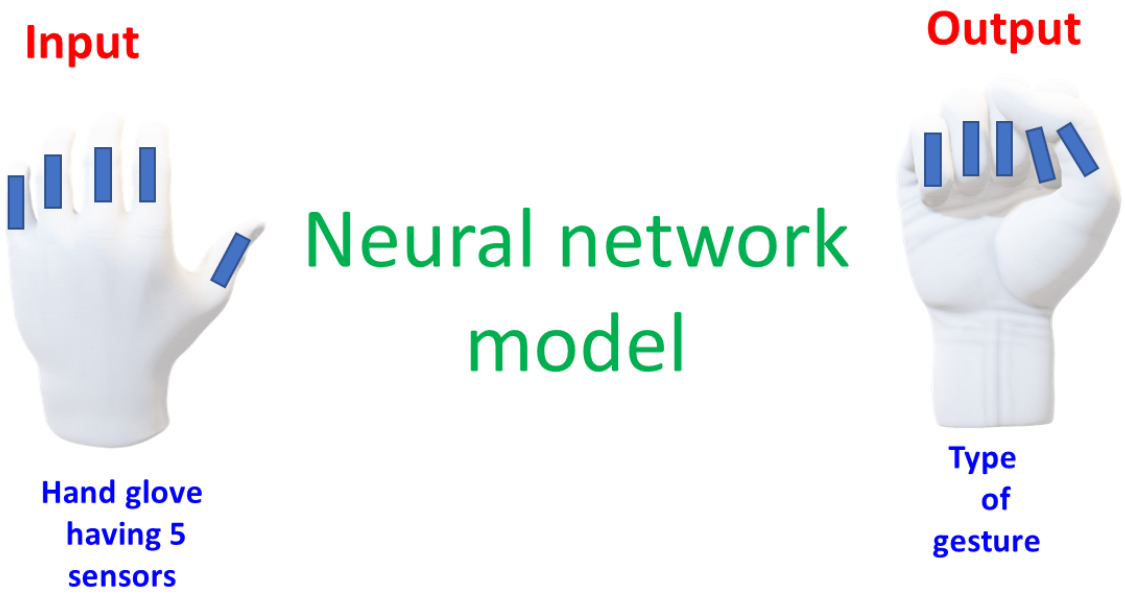

Fig. 1: Schematic diagram for Hand gesture recognition using neural network model

In chapter 5 we have collected data for open hand and fist type of gesture. This sensor data with some modifications can be used for hand gesture recognition for open and fist hand gesture in general. In future sensor data can be collected for both gesture (open hand and fist gesture) on different people (male and female as well) and time recording the data can also be increased for increasing the accuracy. Further with the help of neural network model (as shown in block diagram below) we can label the data and can easily generalize the hand gesture prediction for open and fist gesture. Similarly, some other hand gesture like victory sign or thumbs up etc. can also be performed using various machine learning models.

About the author

NITIN KUMAR SINGH

nitinmjpruiitp@gmail.com

Nitin Kumar Singh was born in Nagariya Satan, Post-Aonla, District-Bareilly, Uttar Pradesh, India. He received his bachelor of technology degree in Electrical Engineering from the Institute of Engineering and Technology, M.J.P. Rohilkhand University, Bareilly, India in 2009. After that he completed his master of technology in Mechatronics from Indian Institute of Technology, Patna, India in 2014. Currently, he is MEXT supported doctoral student pursuing for Ph.D. degree from the Graduate School of Life Science and Systems Engineering of Kyushu Institute of Technology, Japan. During his PhD tenure He also did Internship in AI and data science department at OMRON corporation, Kyoto, Japan. His research area includes application of electroactive polymers, soft and flexible devices, robotics, mechatronics, artificial intelligence in healthcare and biomedical fields, machine learning and deep learning, Data science, Computer vision.

Publications:

1. Singh, Nitin Kumar, Kazuto Takashima, and Shyam S. Pandey. "Fabrication, characterization and modelling of the fabric electrode-based highly stretchable capacitive strain sensor." Materials Today Communications (2022): 104095. https://doi.org/10.1016/j.mtcomm.2022.104095

2. Singh, Nitin Kumar, Kazuto Takashima, and Shyam Sudhir Pandey. "Electronic versus Ionic Electroactive Polymers (EAPs) Strain Sensors for Wearable Electronics: A

Comparative Study." Engineering Proceedings 21.1 (2022): 1. https://doi.org/10.3390/engproc2022021001

3. **Nitin Kumar Singh,** Kazuto Takashima, Shyam S. Pandey, "Tear strength estimation of electroactive polymer-based strain sensors"; **Proc. SPIE 12042, Electroactive Polymer Actuators and Devices (EAPAD) XXIV**, 1204217 (20 April 2022); https://doi.org/10.1117/12.2627807 (5 pages).

4. **Nitin Kumar Singh,** Kazuto Takashima, Shyam S. Pandey, "Fatigue life prediction of electroactive polymer strain sensor **Proc. SPIE 11587, Electroactive Polymer Actuators and Devices (EAPAD) XXIII**, 115871Z (22 March 2021). DOI: https://doi.org/10.1117/12.2584521 (7 pages).

5. **Nitin Kumar Singh,** Kazuto Takashima, Tomohiro Shibata. "Dielectric elastomer based stretchable textile sensor for capturing motion, **Proc. SPIE 11375, Electroactive Polymer Actuators and Devices (EAPAD) XXII**, 113752L, (23 April 2020). DOI: https://doi.org/10.1117/12.2565743 (8 pages).

6. **Nitin Kumar Singh,** Kazuto Takashima, Shyam S. Pandey, Electrical characterization and analytical modeling for predicting stress-strain behavior of electroactive polymer-based sensor under multiaxial loads, 8th International Conference on Sensors and Electronic Instrumentation Advances (SEIA' 2022), 21-23 September 2022 Corfu holiday palace, Corfu, greece (3 pages) https://www.sensorsportal.com/SEIA_2022/SEIA_2022_Proceedings.pdf

Appendix

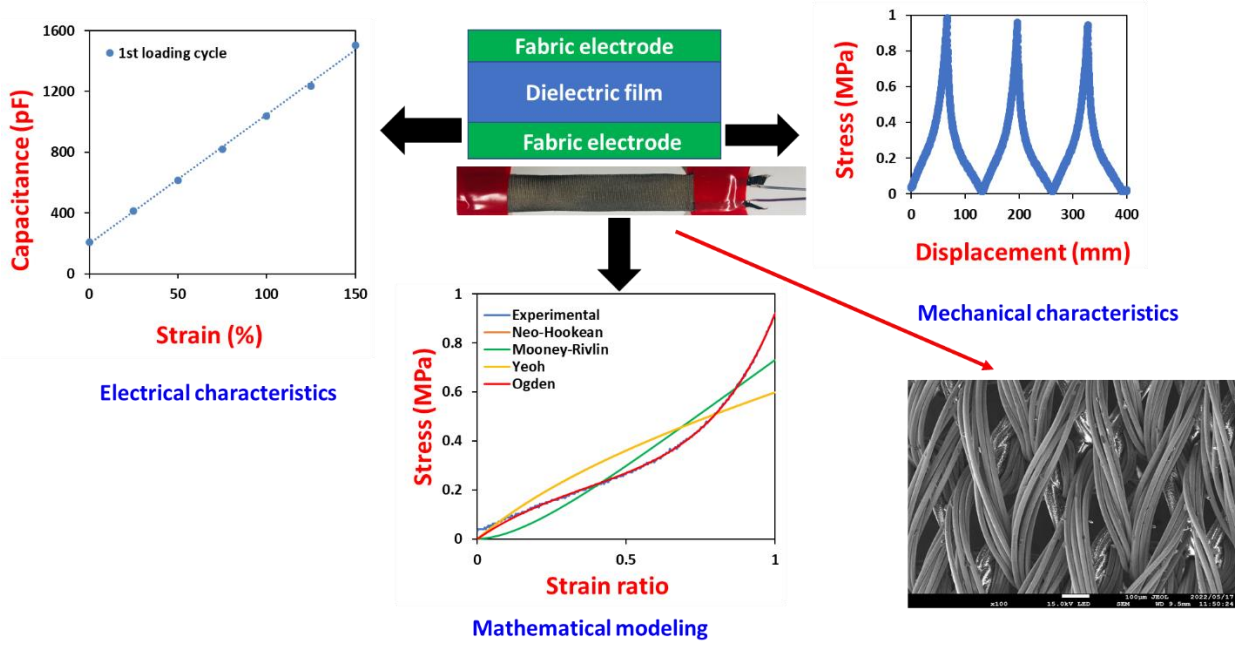
1st loading cycle
Capacitance (pF)
Strain (%)
Electrical characteristics
Fabric electrode
Dielectric film
Fabric electrode
Stress (MPa)
Displacement (mm)
Mechanical characteristics
Experimental
Neo-Hookean
Mooney-Rivlin
Yeoh
Ogden
Stress (MPa)
Strain ratio
Mathematical modeling